WILEY

Traffic flow control on cascaded roads by event-triggered output feedback

Nicolas Espitia[1] | Jean Auriol[2] | Huan Yu[3] | Miroslav Krstic[4]

[1]CRIStAL - Centre de Recherche en Informatique Signal et Automatique de Lille, Univ. Lille, CNRS, Centrale Lille, UMR 9189, Lille, France

[2]L2S-Laboratoire des Signaux et Systèmes, Université Paris-Saclay, CNRS, CentraleSupélec, Gif-sur-Yvette, France

[3]Intelligent Transportation Thrust, Systems Hub, Hong Kong University of Science and Technology, Guangzhou, China

[4]Department of Mechanical and Aerospace Engineering, University of California, San Diego, La Jolla, California, USA

Correspondence
Nicolas Espitia, CRIStAL - Centre de Recherche en Informatique Signal et Automatique de Lille, Univ. Lille, CNRS, Centrale Lille, UMR 9189, F-59000 Lille, France.
Email: nicolas.espitia-hoyos@univ-lille.fr

Abstract

In this article, we propose an event-triggered output-feedback controller that guarantees the simultaneous stabilization of traffic flow on two connected roads. The density and velocity traffic dynamics are described with the linearized Aw-Rascle-Zhang macroscopic traffic partial differential equation model, which results in a coupled hyperbolic system. The control objective is to simultaneously stabilize the upstream and downstream traffic to a given spatially uniform constant steady-state that is in the congested regime. To suppress stop-and-go traffic oscillations on the cascaded roads, we consider a ramp metering strategy that regulates the traffic flow rate entering from the on-ramp to the mainline freeway. The ramp metering is located at the outlet with only boundary measurements of flow rate and velocity. Under the event-triggered scheme, the control signal is only updated when an event triggering condition is satisfied. Compared with the continuous input signal, the event-triggered boundary output control presents a more realistic setting to implement by ramp metering on a digital platform. The event-triggered control design relies on the emulation of the backstepping boundary output feedback and on a dynamic event-triggered strategy to determine the time instants at which the control value must be updated. We prove that there is a uniform minimal dwell-time (independent of initial conditions), thus avoiding the Zeno phenomenon. We guarantee the exponential convergence of the closed-loop system under the proposed event-triggered control. A numerical example illustrates the results.

KEYWORDS

backstepping control design, event-triggered control, PDE-based control, ramp metering, traffic flow model

1 | INTRODUCTION

Freeway traffic modeling and management have been intensively investigated due to the increasing demand for traffic mobility over the past decades. Various traffic control methods have been studied to regulate freeway traffic systems and mitigate traffic congestion. In particular, stop-and-go traffic is a common phenomenon appearing on congested freeways. In congested traffic, drivers are forced into the acceleration-and-deceleration cycles. Such oscillations and causes characterize the stop-and-go traffic, increased consumption of fuel, and unsafe driving conditions.

Among different models for freeway traffic, macroscopic modeling is particularly suitable to describe the stop-and-go traffic since the propagation of traffic waves is described in the temporal and spatial domain. The macroscopic models use hyperbolic partial differential equations (PDEs) that govern the evolution of traffic density and velocity dynamics. The most widely-used macroscopic traffic PDE models include the classical first-order Lighthill-Whitham-Richards (LWR) model[1,2] and the state-of-art second-order Aw-Rascle-Zhang (ARZ) model.[3,4] The LWR model corresponds to the conservation law of traffic density. Although it can efficiently predict the formation and propagation of traffic shockwaves on the freeway, it does not succeed in describing the stop-and-go oscillatory phenomenon.[5] As this may cause unsafe driving conditions, increased fuel consumption, and delays in travel time, the second-order Aw-Rascle-Zhang (ARZ) model[3,4] seems more suitable since this model manages to describe this stop-and-go traffic congestion by allowing a velocity PDE added to the LWR model and thus providing a wider variety of dynamics. This model describes the traffic density and velocity of a freeway segment with two coupled non-linear hyperbolic PDEs. Developed initially to describe the traffic flow on a single road, this class of models has been extended in References 6,7 to describe the freeway traffic on complex road network structures. In this work, we consider a network composed of two cascaded freeway segments (that may have different intrinsic properties). Thus, we adopt the second-order macroscopic traffic network model in Reference 7 for the two cascaded freeway segments. In particular, we assume that there is a conservation of the mass and drivers' properties at the junction connecting the two roads. This property is not smooth across the junction in Reference 6. The well-posedness of a closed-loop system for our control design is a consequence of the fact that the solution in Reference 7 is a weak solution in the sense of the conservative variables of the ARZ model. All in all, the system under consideration can be expressed as a network of two interconnected hyperbolic PDE systems coupled through their boundaries. We are interested in developing control strategies to mitigate stop-and-go oscillations.

To regulate freeway traffic and avoid the stop-and-go oscillatory phenomenon, different traffic control strategies have been developed in the literature. They are mainly implemented on the traffic management infrastructures, that is, ramp metering and varying speed limits (VSL). Ramp metering controls the traffic lights on a ramp such that the inflow traffic is regulated for the mainline traffic. The VSL regulates traffic velocity by displaying driving velocities that are time-varying and dependent on real-time traffic. A complete survey on freeway traffic control can be found in Reference 8. Boundary control algorithms have been developed for traffic control of a single freeway segment in References 9-12. However, these control laws are restricted to control problem of traffic on one freeway segment which necessitates certain road homogeneity. A first research line aimed at the definition of feedback approaches for speed control of freeway traffic streams. In Reference 10, the authors design a control law that depends on measurements of a portion of the system state and that is integrated in a LWR model. In Reference 12 or 13, the authors design PI boundary control of a cascaded freeway network, which is modeled by the linearized homogeneous AR model. The static errors of boundary conditions are suppressed since the instabilities do not arise from the transport PDEs. The proposed controllers have been tested against traffic experiment in Reference 13 that suggests that the proposed strategy is feasible and effective. The present paper differs in focusing on the oscillations generated by the in-domain traffic that can only be modeled by the inhomogeneous ARZ model. Moreover, all the boundaries of the network are actuated in References 12,13 which is not the case in this work, where we only consider that one boundary of the network is actuated. In Reference 14, the authors have proposed a control algorithm based on time-gap setting of ACC equipped and connected vehicles in-domain actuation. Optimal control of traffic networks modeled by means of PDEs are reported in Reference 15. Finally, the backstepping approach provides an effective way to design stabilizing controllers for the considered class of systems. A ramp metering control strategy has for instance been proposed in Reference 11 to suppress the stop-and-go traffic oscillations on the freeway either upstream or downstream of the ramp, based on the theoretical result developed in References 16-18. A related backstepping-based state-observer has been tested in Reference 19 on field data. However, such control design can not stabilize the two segments simultaneously, and distinct traffic scenarios appearing on the cascaded segments are not addressed by the model. Ramp metering control of the upstream traffic may cause congestion for downstream traffic and vice versa. This problem has only been overcome recently since an output-feedback control law (based on boundary measurement) that simultaneously stabilizes the traffic on two cascaded road segments has been designed in Reference 20. The proposed strategy required rewriting the network as an underactuated fourth-order PDE system and applying recent theoretical developments obtained thanks to the backstepping approach.[21]

Nevertheless, the continuous boundary control and estimation strategies developed for the traffic problem need to be implemented into digital platforms. For instance, in ramp metering control strategies, the rate inflow is controlled through traffic lights modulation that cannot be carried out continuously. Typically, periodic strategies are used to modulate the frequency of light changes. In VSL strategies, on the other hand, it is not feasible to display continuous time-varying driving speed advisories. It has to be done either periodically or on events. The drawback with periodic

implementations is that one may produce unnecessary updates of the controllers which may cause over utilization of computational/communication resources, actuator changes that are more frequent than necessary and unsafe driving conditions. Therefore, for the arising continuous time boundary controllers, the issue of sampling has to be carefully studied. Indeed, if sampling is not addressed properly, the stability and estimation properties may be lost. Therefore, sampled-data and event-triggered control can offer suitable approaches to be adopted towards digital realizations.

Few approaches on sampled-data and event-triggered control of parabolic PDEs are considered in References 22,23 and 24-30. For abstract distributed parameter systems sampled-data control is investigated in References 31 and 32. For hyperbolic PDEs, sampled-data control is studied in References 33 and 34 and event-triggered control in References 35-37 and in References 38 and 39 for coupled hyperbolic PDE-ODEs. It is worth saying that the event-triggered strategies in the infinite dimensional setting have been inspired by some of those already well-established for finite-dimensional systems, see for example, References 40-46 and the references therein.

Moreover, event-triggered control strategies applied to traffic flow have been proposed namely for freeway discrete-time models (e.g., those coming from the Cell Transmission Model (CTM) where subdivision of the freeway into cells and the discretization of the time horizon are typically done). They are suitable for implementation-oriented control design: for example, using Model Predictive Control (MPC) combined with event-triggered control to determine the ramp metering actions, as it is proposed in Reference 47 and later in Reference 48 for MPC networked scheme which accounts also for event-triggering the state information measured by sensors. Then, hierarchical event-triggered control schemes for multi-class traffic networks scheme have been designed in Reference 49. On the whole, event-triggered model predictive control clearly shows to be more efficient than solely MPC strategies, especially when reducing the frequency in solving the optimization problem and hence updating the control laws only when needed. Unlike these works which rely on the emulation of ramp metering controllers and that build on discrete-time system (finite-dimensional system), the first event-triggered backstepping-based boundary control strategy has been proposed in Reference 50 for varying speed limit (VSL) to reduce the stop-and-go traffic oscillations. The controlled velocity signal is only updated when an event triggering condition is satisfied. It builds on the linearized ARZ traffic modeled and the emulation is done for a continuous-time boundary controller (which is designed under a late-lumped approach, thus without any type of model reduction).

The novelty of this article consists of the design of an event-triggered output-feedback law that stabilizes the traffic on two cascaded road segments for which actuation is implemented at the outlet with ramp metering. The associated measurement corresponds to the values of the traffic states at the outlet. The contributions of this article are threefold: (1) From a theoretical point of view, this article is the first attempt to design an observer-based event-triggered control law for an underactuated hyperbolic system; (2) We apply the proposed event-triggered strategy to the challenging problem of traffic networks, thus avoiding useless actuation solicitations and making possible real implementation. The proposed event-triggered algorithm is based on the emulation of the output-feedback law designed in Reference 20, to which an event-triggered mechanism (including a dynamic triggering condition) is added. (3) We show the Zeno phenomenon's avoidance and the closed-loop system's exponential convergence (in the sense of the L^2-norm) with the proposed control law. To show the closed-loop convergence and the avoidance of the so-called Zeno phenomenon (which would made implementation impossible), the proposed strategy combines the backstepping methodology with a Lyapunov analysis. More precisely, using several backstepping transformations, the closed-loop system is mapped to simpler target systems that corresponds to cascaded system of conservation laws subject to the action of a disturbance at its boundary. This disturbance can be viewed as an actuation deviation between the continuous (nominal) controller designed in Reference 20 and the event-triggered one. From this target system, we can perform a Lyapunov analysis to analyze the growth-in-time of the deviation $d(t)$ and show the avoidance of the Zeno-phenomenon and the closed-loop convergence. Preliminary results related to this work have been presented in Reference 51.

The article is organized as follows. In Section 2, we present the ARZ PDE model we use to describe the road network we consider in this article. It consists of two connected road segments with unidirectional traffic flow and different road conditions. Part of the content of this section is borrowed from Reference 20. After folding and rescaling transformations, this PDE system is expressed as a 2+2 hyperbolic system for which only one equation is actuated at the boundary. In Section 3, we present the nominal output-feedback law that has been designed in Reference 20. We introduce several backstepping transformations that are useful for the analysis. Finally, we emulate this continuous control law using a discretized event-triggered version: the control value is held constant between two successive time instants and is updated when some triggering condition is verified. The dynamic triggering condition is presented in Section 4. We show in Section 5 the avoidance of the Zeno phenomenon and the exponential convergence of the closed-loop system in the sense of the L^2-norm. Some simulation results are presented in Section 6. Finally, we give some concluding remarks in Section 7.

Notations

For any $(a, b) \in \mathbb{R}^2$, we denote $L^2([a, b], \mathbb{R})$ the space of real-valued square-integrable functions defined on $[a, b]$ with the standard L^2-norm, that is, for any $f \in L^2([a, b], \mathbb{R})$, $||f||^2_{L^2([a,b])} := \int_a^b f(x)^2 dx$. When there is no ambiguity on the integration domain, the sub-index $L^2([a, b])$ will be omitted. For any function of two variables $f(x, t)$ defined on $x \in [a, b]$, $t \in [0, \infty)$, the spatial L^2-norm is the function $||f||^2_{L^2([a,b])}$ defined as $||f||^2_{L^2([a,b])}(t) := \int_a^b f(x, t)^2 dx$.

For any bounded set $\mathcal{T}$ of $\mathbb{R}^2$, we denote $\mathcal{B}(\mathcal{T})$ the set of bounded real functions on $\mathcal{T}$. This set is a Banach space for the sup-norm. We define the sets $\mathcal{T}_1, \mathcal{T}_2$ as follows:

$$\mathcal{T}_1 = \{(x, \xi) \in [0, L]^2, \xi \geq x\}, \quad \mathcal{T}_2 = \{(x, \xi) \in [0, L]^2, \xi \leq x\}, \tag{1}$$

and, the set $\mathcal{T}_3$ is defined as the unit square $[0, L]^2$: $\mathcal{T}_3 = \{(x, \xi) \in [0, L]^2\}$. The set $\mathcal{T}_1$ is the upper-part of this square while $\mathcal{T}_2$ corresponds to its lower part.

2 | PRELIMINARIES AND PROBLEM DESCRIPTION

As in Reference 20, we consider a road network that consists of two connected road segments with unidirectional traffic flow and different road conditions, as shown in Figure 1. The two segments are assumed to have the same length L for simplicity of notation. The spatial scaling can be easily made for equations that are used to describe traffic states on segments with different lengths. The first segment (downstream segment) is defined on $[0, L]$ while the second segment (upstream segment) is defined on $[-L, 0]$. These two segments are connected at the junction through the boundary $x = 0$. The traffic dynamics are described with the ARZ PDE model and the junction between the two segments is represented with the boundary conditions of the PDE model. The adopted ARZ PDE-based traffic network model by Herty and Rascle[7] allows the existence of weak solutions, which we will define later for the open-loop and closed-loop system. The evolution of traffic density $\rho_1(t, x)$ and velocity $v_1(t, x)$ (with $(t, x) \in [0, \infty) \times [0, L]$) on the downstream road segment and traffic density $\rho_2(t, s)$ and velocity $v_2(t, s)$ ($(t, s) \in [0, \infty) \times [-L, 0]$) on the upstream road segment are modeled by the following ARZ model.

$$\partial_t \rho_i + \partial_x (\rho_i v_i) = 0, \tag{2}$$

$$\partial_t (\rho_i (v_i + p_i)) + \partial_x (\rho_i v_i (v_i + p_i)) = -\frac{\rho_i (v_i - \mathcal{V}_i (\rho_i))}{\tau_i}, \tag{3}$$

where $i \in \{1, 2\}$ represents downstream and upstream road respectively. The labeling of freeway segments is chosen as the reverse direction of traffic flow but same as the propagation direction of the control signal, which will be explained later. The traffic pressure $p_i (\rho_i)$ is defined as an increasing function of the density $p_i (\rho_i) = v_m \rho_i^{\gamma_i} / \rho_{m,i}^{\gamma_i}$. The coefficient γ_i represents the overall drivers' property, reflecting their change of driving behavior to the increase of density. The positive constant v_m represents the maximum velocity and the positive constant $\rho_{m,i}$ is the maximum density defined as the number of vehicles per unit length. The equilibrium density-velocity relation $\mathcal{V}_i (\rho_i)$ is given by $\mathcal{V}_i (\rho_i) = v_m - p_i (\rho_i)$ for
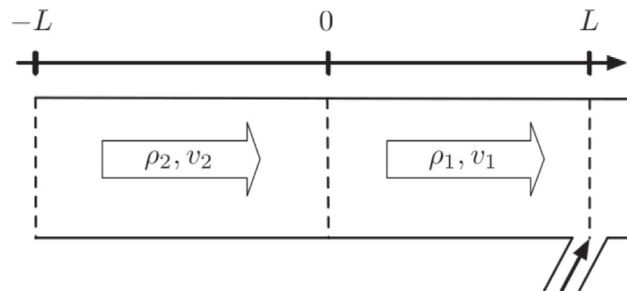

FIGURE 1 Traffic flow on an incoming road and an outgoing road connected with a junction. Actuation is implemented at the outlet with ramp metering
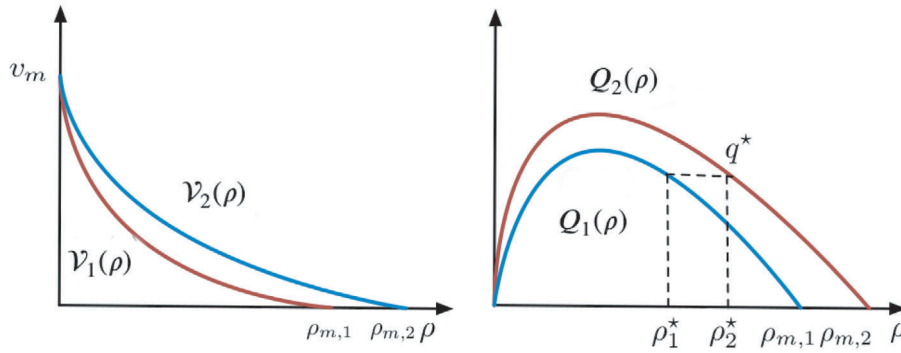
FIGURE 2 The equilibrium density and velocity relation $\mathcal{V}_i(\rho)$ on the left, the equilibrium density and flux relation $Q_i(\rho)$ on the right

both segments, which assumes the same maximum velocity for the two segments when there are no vehicles on the road $\rho_i = 0$. We define the following variable

$$w_i = v_i + p_i(\rho_i), \tag{4}$$

which is interpreted as traffic "friction" or drivers' property.[52] This property transports in the traffic flow with vehicle velocity, representing the heterogeneity of individual driver with respect to the equilibrium density-velocity relation $\mathcal{V}_i(\rho_i)$. The maximum velocity v_m is assumed to be the same for the two road segments while the maximum density $\rho_{m,i}$ and coefficient γ_i are allowed to vary. The positive constant τ_i is the relaxation time that represents the time scale for traffic velocity v_i adapting to the equilibrium density velocity relation $\mathcal{V}_i(\rho_i)$.

We denote the traffic flow rate on each road as $q_i = \rho_i v_i$. The equilibrium flow and density relation, also known as the fundamental diagram, is then given by $Q_i(\rho_i) = \rho_i \mathcal{V}_i(\rho_i) = \rho_i v_m \left(1 - (\rho_i/\rho_{m,i})^{\gamma_i}\right)$. We assume that the equilibrium traffic relation is different for the two segments due to the change of road situations and access to road junction. The illustration is given in Figure 2. The critical density ρ_c splits the free and congested regimes of traffic states. The critical density is given by $\rho_{c,i} = \rho_{m,i}/(1 + \gamma_i)^{1/\gamma_i}$ such that $Q_i'(\rho_i)\big|_{\rho_i = \rho_{c,i}} = 0$. For a section i, the traffic is free when the density satisfies $\rho_i < \rho_{c,i}$. The traffic is defined as the congested one when the density satisfies $\rho_i > \rho_{c,i}$. For the free traffic, oscillations around the steady states will be damped out fast. For the congested traffic, there are two directional waves on road with one being the velocity oscillation propagating upstream and the other one being the density oscillation propagating downstream with the traffic. The congested traffic can become unstable.[53] We consider the situation that the upstream road segment 2 for $s \in [-L, 0]$ has more lanes than the downstream road segment for $x \in [0, L]$, in which congested traffic is usually formed up from downstream to upstream. Therefore, the maximum density $\rho_{m,2} > \rho_{m,1}$. The maximum driving speed v_m is assumed to be the same for the two segments. The maximum flow rate of the upstream road $Q_2(\rho_c)$ is reduced in the downstream to $Q_1(\rho_c)$, due to the change of road conditions from segment 2 to segment 1.

2.1 | Actuated boundary

For the boundary conditions connecting the two PDE systems, the Rankine–Hugoniot condition is satisfied at the junction such that the weak solution exists for the network (2)–(3). This condition implies piecewise smooth solutions and corresponds to the conservation of the mass and of the drivers' properties defined in (4) at the junction. Thus the flux and drivers' property are assumed to be continuous across the boundary conditions at $x = 0$, that is

$$\rho_1(t, 0)v_1(t, 0) = \rho_2(t, 0)v_2(t, 0), \tag{5}$$

$$w_1(t, 0) = w_2(t, 0). \tag{6}$$

For the open-loop system, we assume a constant inflow $q^\star$ entering the inlet boundary $s = -L$ and a constant outflow $q^\star$ at the outlet boundary for $x = L$:

$$q_2(t, -L) = q^\star, \tag{7}$$

$$q_1(t, L) = q^\star. \tag{8}$$

The control problem we solve consists in stabilizing on events the traffic flow in both the upstream and downstream road segments with a single actuator. Three possible locations for implementing a ramp metering control input are either at the inlet $x = -L$, at the junction $x = 0$ or at the outlet $x = L$ as in Reference 20. However, in this article we only present the observer-based event triggered control results for control input acting on the outlet and that is updated according to a suitable event-triggering condition. Note that the other cases could be solved adjusting the proposed techniques.

Ramp metering control $U_{\text{nom}}(t)$ from the outlet $x = L$: The downstream outflow at $x = L$ is actuated by $U_{\text{nom}}(t)$,

$$q_1(t, L) = q^\star + U_{\text{nom}}(t), \tag{9}$$

where the outflow rate equals the summation of the onramp metering flow and the constant mainline flow. The designed controller U_{nom} is the flow rate perturbation around a nominal flow rate. We assume that the steady-state flow rate consists of a nominal onramp flow rate $q_r \geq 0$, which is a component of the steady-state flow rate $q^\star$. Then the actual ramp flow input at an onramp is given by

$$q_{\text{ramp}}(t) = q_r + U_{\text{nom}}(t) \geq 0. \tag{10}$$

In practice, we only need to guarantee that $q_{\text{ramp}}(t)$ is non-negative so that $U_{\text{nom}}(t) \geq -q_r$. The value of q_r depends on the road configuration and real-time traffic conditions. We assume that there exists $q_r > 0$ such that (10) always holds.

2.2 | Congested steady states $\left(\rho_1^\star, v_1^\star, \rho_2^\star, v_2^\star \right)$

We are concerned with the congested traffic and assume that the equilibrium of both segments $(\rho_1^\star, v_1^\star)$, $(\rho_2^\star, v_2^\star)$ are in the congested regime, which is the only one of theoretical control interest among all four traffic scenarios including free and free, free and congested, congested and free, congested and congested. If the traffic of both segments is free, there is no need for ramp metering control. If the upstream segment 2 is in the free regime and the downstream segment 1 is congested, then we only need to control the congested downstream traffic with $U_{\text{nom}}(t)$ as presented in Reference 11. The oscillations propagated from the congested segment to the free regime segment will be damped out soon. The same applies to the scenario of free traffic in downstream segment 1 and congested traffic in upstream segment 2. The control objective is to stabilize the traffic flow in the two segments around the steady states. In practice, the steady states represent the equilibrium state values of the traffic flow when oscillations are successfully suppressed by our control design.

The steady states $(\rho_1^\star, v_1^\star)$, $(\rho_2^\star, v_2^\star)$ are considered to be in the congested regime and the boundary conditions (5) and (6) are satisfied, that is,

$$\rho_1^\star v_1^\star = \rho_2^\star v_2^\star = q^\star, \tag{11}$$

$$w_1^\star = w_2^\star = v_m, \tag{12}$$

where the steady state velocities satisfy the equilibrium density-velocity relation $v_i^\star = \mathcal{V}_i\left(\rho_i^\star\right)$, as shown in Figure 2. According to (4) the constant driver's property in (12) implies that we have the same maximum velocity v_m for the two segments (which corresponds to our initial assumption):

$$v_1^\star + p_1^\star = v_2^\star + p_2^\star = v_m, \tag{13}$$

where $p_i^\star = p_i\left(\rho_i^\star\right)$. The steady states can be solved from the above nonlinear equations (11), (13) however there are no explicit solutions. Therefore we show the derivation process for obtaining the steady state values when $\rho_1^\star$ and the model parameters v_m, $\rho_{m,i}$, and γ_i are given. The functions $\mathcal{V}_i(\rho) Q_i(\rho)$, and $p_i(\rho)$ are also known. The steady state flow rate in (11) is obtained as $q^\star = Q_1\left(\rho_1^\star\right)$, and the constant flux $Q_1\left(\rho_1^\star\right) = Q_2\left(\rho_2^\star\right)$, yields a relation for the steady state densities of the two segments $\frac{\rho_1^\star \rho_{m,1}^{\gamma_1} - \left(\rho_1^\star\right)^{\gamma_1+1}}{\rho_2^\star \rho_{m,2}^{\gamma_2} - \left(\rho_2^\star\right)^{\gamma_2+1}} = \frac{\rho_{m,1}^{\gamma_1}}{\rho_{m,2}^{\gamma_2}}$. Knowing $\rho_1^\star$, $\rho_2^\star$, and $q^\star$, the steady states velocities are obtained as $v_i^\star = q^\star / \rho_i^\star$.

2.3 | Linearized ARZ model in Riemann coordinates

We linearize the ARZ based traffic network model (ρ_i, v_i) in (2), (3) with the boundary conditions (5)–(8) around the steady states $(\rho_i^\star, v_i^\star)$ defined in the previous section. In order to simplify the control design, the linearized model is then rewritten into the Riemann variables to which we apply an invertible spatial transformation

$$\overline{w}_i = \exp\left(\frac{x}{\tau_i v_i^\star}\right)\left(\frac{\gamma_i p_i^\star}{q^\star}\left(\rho_i v_i - \rho_i^\star v_i^\star\right) + \frac{1}{r_i}\left(v_i - v_i^\star\right)\right), \tag{14}$$

$$\overline{v}_i = v_i - v_i^\star, \tag{15}$$

$$\overline{q}_i = \rho_i v_i - \rho_i^\star v_i^\star, \tag{16}$$

where $p_i^\star = p_i\left(\rho_i^\star\right)$ and the constant coefficients r_i are defined as

$$r_i = -\frac{v_i^\star}{\gamma_i p_i^\star - v_i^\star}. \tag{17}$$

For the congested regime we have $\rho_i^\star > \frac{\rho_{m,i}}{(1+\gamma_i)^{1/\gamma_i}}$ so that the characteristic speed $\gamma_i p_i^\star - v_i^\star > 0$. The velocity variations $\overline{v}_1(t,x)$, $\overline{v}_2(t,x)$ transport upstream which means the action of velocity acceleration or deceleration is repeated from the leading vehicle to the following vehicle. More precisely, since $v_i^\star = v_m - p_i^\star$, we obtain $\gamma_i p_i^\star - v_i^\star = (1 + \gamma_i)p_i^\star - v_m$. We also have $p_i^\star = v_m - \mathcal{V}_i\left(\rho_i^\star\right) = v_m\left(\frac{\rho_i^\star}{\rho_{m,i}}\right)^{\gamma_{v_m}} > \frac{v_m}{1+\gamma_i}$, since $\rho_i^\star > \frac{\rho_{m,i}}{(1+\gamma_i)^{1/\gamma_i}}$. Consequently, we obtain $\gamma_i p_i^\star - v_i^\star > 0$.

The linearized system with the controlled boundary condition (9) is written as

$$\partial_t \overline{w}_1(t,x) + v_1^\star \partial_x \overline{w}_1(t,x) = 0, \tag{18}$$

$$\partial_t \overline{v}_1(t,x) - (\gamma_1 p_1^\star - v_1^\star)\partial_x \overline{v}_1(t,x) = \overline{c}_1(x)\overline{w}_1(t,x), \tag{19}$$

$$\partial_t \overline{w}_2(t,s) + v_2^\star \partial_s \overline{w}_2(t,s) = 0, \tag{20}$$

$$\partial_t \overline{v}_2(t,s) - (\gamma_i p_2^\star - v_2^\star)\partial_s \overline{v}_2(t,s) = \overline{c}_2(s)\overline{w}_2(t,s), \tag{21}$$

with boundary conditions,

$$\overline{w}_1(t,0) = \overline{w}_2(t,0), \tag{22}$$

$$\overline{v}_1(t,L) = r_1 \exp\left(\frac{-L}{\tau_1 v_1^\star}\right)\overline{w}_1(t,L) + \frac{1-r_1}{\rho_1^\star}U_{\text{nom}}(t), \tag{23}$$

$$\overline{w}_2(t,-L) = \frac{1}{r_2}\exp\left(\frac{-L}{\tau_2 v_2^\star}\right)\overline{v}_2(t,-L), \tag{24}$$

$$\overline{v}_2(t,0) = \delta\frac{r_2}{r_1}\overline{v}_1(t,0) + (1-\delta)r_2\overline{w}_2(t,0), \tag{25}$$

where $s \in [-L, 0]$, $x \in [0, L]$, and where the spatially varying coefficient $\overline{c}_1(x)$, $\overline{c}_2(s)$ are defined, respectively, by

$$\overline{c}_1(x) = -\frac{1}{\tau_1}\exp\left(-\frac{x}{\tau_1 v_1^\star}\right), \quad \overline{c}_2(s) = -\frac{1}{\tau_2}\exp\left(\frac{s}{\tau_2 v_2^\star}\right). \tag{26}$$

The constant coefficient δ (ratio related to the traffic pressure of the segments) is defined by

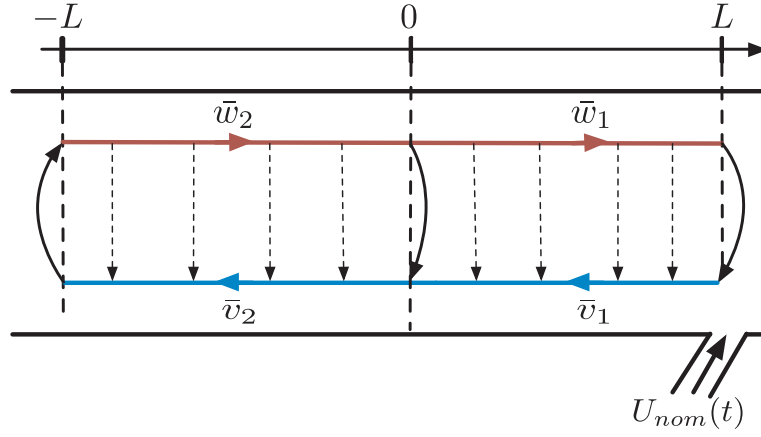$$\delta = \frac{\gamma_2 p_2^\star}{\gamma_1 p_1^\star}. \tag{27}$$

FIGURE 3 Traffic flow on an incoming road and an outgoing road connected with a junction. Actuation is implemented at the outlet with ramp metering

Although the cascade structure of the network given Figure 3 presents some advantages for the design of a stabilizing control law (see Reference 20), it is more convenient for the design of an event-triggered algorithm to have all the states defined on the same spatial domain. Therefore, to rewrite the states $\bar{w}_2$ and $\bar{v}_2$ as functions defined on $[0, L]$, we consider the *folding transformation* $\bar{x} = -s$. The variable $\bar{x}$ belongs to $[0, L]$. For sake of simplicity, we will omit the bar and abusively denote $\bar{w}_2(t, \bar{x}) = \bar{w}_2(t, x)$. With this transformation, the previous system rewrites

$$\partial_t \bar{w}_1(t, x) + v_1^\star \partial_x \bar{w}_1(t, x) = 0, \tag{28}$$

$$\partial_t \bar{v}_2(t, x) + (\gamma_2 p_2^\star - v_2^\star) \partial_x \bar{v}_2(t, x) = c_2(x) \bar{w}_2(t, x), \tag{29}$$

$$\partial_t \bar{v}_1(t, x) - (\gamma_1 p_1^\star - v_1^\star) \partial_x \bar{v}_1(t, x) = c_1(x) \bar{w}_1(t, x), \tag{30}$$

$$\partial_t \bar{w}_2(t, x) - v_2^\star \partial_x \bar{w}_2(t, x) = 0, \tag{31}$$

where $x \in [0, L]$, and $c_1(x) = \bar{c}_1(x)$ and $c_2(x) = \bar{c}_2(-x)$. The boundary conditions are,

$$\begin{pmatrix} \bar{w}_1(t, 0) \\ \bar{v}_2(t, 0) \\ \bar{v}_1(t, L) \\ \bar{w}_2(t, L) \end{pmatrix} = G \begin{pmatrix} \bar{w}_1(t, L) \\ \bar{v}_2(t, L) \\ \bar{v}_1(t, 0) \\ \bar{w}_2(t, 0) \end{pmatrix} + \begin{pmatrix} 0 \\ 0 \\ \frac{1-r_1}{\rho_1^\star} \\ 0 \end{pmatrix} U_{\text{nom}}(t), \tag{32}$$

where

$$G = \begin{pmatrix} 0 & 0 & 0 & 1 \\ 0 & 0 & \delta \frac{r_2}{r_1} & (1-\delta) r_2 \\ r_1 \exp\left(\frac{-L}{\tau_1 v_1^\star}\right) & 0 & 0 & 0 \\ 0 & \frac{1}{r_2} \exp\left(\frac{-L}{\tau_2 v_2^\star}\right) & 0 & 0 \end{pmatrix}. \tag{33}$$

The schematic representation of the interconnected system (28)–(32) is given in Figure 4. The open-loop system (28)–(32) (for which $U_{\text{nom}} \equiv 0$) is well-posed in the sense of the L^2 norm (weak solutions) by Bastin and Coron[9(theorem A.4)], that is, for any initial conditions $((\bar{v}_0)_i, (\bar{w}_0)_i) \in (L^2([0, L]))^2$, there is only one L^2-solution. It is shown in Reference 11 that only marginal linear stability holds for the open-loop system of one segment. The control operator is admissible (i.e., it verifies the so-called admissibility condition as stated in Reference 54). Consequently, for any $U_{\text{nom}} \in L^2([0, T])$, and for
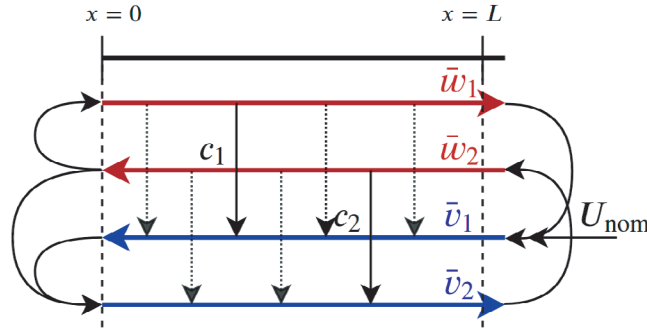
FIGURE 4 Schematic representation of the interconnected system (28)–(32) after folding transformation. Actuation is implemented at the outlet with ramp metering

any initial conditions $((\overline{v}^0)_i, (\overline{w}^0)_i) \in (L^2([0, L]))^2$ there is only one L^2-solution to (28)–(32) . Note that we could obtain more regular solutions (strong solutions) by imposing some additional regularity conditions on the initial conditions or the coupling terms, and adding compatibility conditions (see Reference 9 for instance). An output-feedback law that exponentially stabilizes (28)–(32) in the sense of the L^2-norm has been designed in Reference 20. We assume that the **available measurements** correspond to the values of $\tilde{q}_i$ and $\tilde{v}_i$ at the left side of the outlet $x = L$. Since we have $\overline{w}_1(t, L) = \exp\left(\frac{L}{\tau_1 v_1^\star}\right)\left(\frac{\gamma_1 p_1^\star}{q^\star}\overline{q}_1(t, L) - \frac{1}{r_1}\overline{v}_1(t, L)\right)$, we can consider that the boundary measurement corresponds to

$$Y_L(t) = \overline{w}_1(t, L). \tag{34}$$

2.4 | Condition for exponential stability of linear hyperbolic systems and assumption to guarantee delay-robust stabilization

It is worth recalling that a sufficient condition for the exponential stability of 1D hyperbolic systems on a bounded interval was derived in Reference 55 (theorem 2.3) by means of Lyapunov techniques. It is often referred to as a *Dissipativity boundary condition*[*]. We recall it here for the case of the linear hyperbolic system (28)–(32) in the absence of in-domain coupling and actuation.

Consider the following norm for the matrix G:

$$\mathcal{S}_1(G) = \inf\{\|\Delta G\Delta^{-1}\|; \Delta \in \mathcal{D}_4^+\},$$

where $\|\cdot\|$ denotes the usual matrix 2-norm and $\mathcal{D}_4^+$ denotes the set of diagonal 4×4 real matrices with strictly positive diagonal entries. If the following inequality holds:

$$\mathcal{S}_1(G) < 1,$$

then, the system (28)–(32) (in the absence of in-domain coupling and actuation) is exponentially stable.

Moreover, it has been proved in Reference 21 (by in turn relying on References 58 and 59) that the stability of the system (28)–(32) in the absence of in-domain coupling and actuation is necessary to design delay-robust control laws. Therefore, in the rest of this article we consider this assumption.

Assumption 1. The boundary conditions of the system (28)–(32) with G given by (33) are dissipative, that is, the following inequality holds:

$$\mathcal{S}_1(G) < 1. \tag{35}$$

2.5 | Control objective

It happens that the in-domain coupling terms $c_i(x)$, $i = 1, 2$ in (28)–(32) (see Figure 4) are the main source of oscillations causing the linearized system to become potentially unstable (or damped with oscillations that take long to settle). The control objective is to suppress the stop-and-go oscillation phenomenon which translates in simultaneously stabilizing

the upstream and downstream traffic to a given spatially uniform constant steady-state. We propose an output-feedback controller located at the outlet of the downstream traffic with collocated sensing of flow rate and velocity at the outlet. The state feedback and observer designs are based on the PDE backstepping methodology aiming at compensating the coupling terms of the under-actuated network of two systems of two hyperbolic PDEs as in (28)–(32). They are adjusted from the one proposed in Reference 20. Considering that the continuous-time boundary control and estimation designs need to be implemented into digital platforms, we develop an event-triggered boundary control law that stabilizes the system on events. The proposed event-triggered controller is piecewise constant. The control value is updated based on a dynamic triggering condition only when needed. The application of such an event-triggered control strategy is the main contribution of this article and is crucial to reduce the computational effort and envision a ramp metering control with modulation of the changing frequency of the on-ramp traffic light. In this article, we consider that the actuator and sensor are colocated at the boundary $x = L$. However, the proposed approach can be extended to the case of in-between measurement/actuation, since the design of the underlying backstepping observers and controllers has already been proposed in Reference 20. Thus, the methodology proposed in Sections 3 and 4 can be easily adjusted to cover these cases.

3 | OUTPUT-FEEDBACK LAW AND EMULATION

3.1 | Output-feedback control law (nominal)

The following output-feedback law $U_{\text{nom}}(t)$ (having delay-robustness margins) has been proposed in Reference 20 to stabilize the system (28)–(32):

$$U_{\text{nom}}(t) = \frac{\rho_1^\star}{1 - r_1} \left(\int_0^L \left(K_1^{vw}(L, \xi)\hat{w}_1(t, \xi)d\xi + K_1^{vv}(L, \xi)\hat{v}_1(t, \xi) + K^w(L, \xi)\hat{w}_2(t, \xi) + K^v(L, \xi)\hat{v}_2(t, \xi) \right) d\xi \right), \quad (36)$$

where the kernels K_1^{vw}, K_1^{vv}, K^w, and K^v are bounded (piecewise continuous) functions that are characterized in Appendix A.3. In addition, $\hat{w}_i$, $\hat{v}_i$ are the states of the following observer relying on the available measurement $Y_L(t) = \overline{w}_1(t, L)$. The observer equations read as follows:

$$\partial_t \hat{w}_1(t, x) + v_1^\star \partial_x \hat{w}_1(t, x) = \mu_1(x)(\hat{w}_1(t, L) - \overline{w}_1(t, L)), \quad (37)$$

$$\partial_t \hat{v}_2(t, x) + (\gamma_2 p_2^\star - v_2^\star)\partial_x \hat{v}_2(t, x) = c_2(x)\hat{w}_2(t, x) + v_2(x)(\hat{w}_1(t, L) - \overline{w}_1(t, L)), \quad (38)$$

$$\partial_t \hat{v}_1(t, x) - (\gamma_1 p_1^\star - v_1^\star)\partial_x \hat{v}_1(t, x) = c_1(x)\hat{w}_1(t, x) + v_1(x)(\hat{w}_1(t, L) - \overline{w}_1(t, L)), \quad (39)$$

$$\partial_t \hat{w}_2(t, x) - v_2^\star \partial_x \hat{w}_2(t, x) = \mu_2(x)(\hat{w}_1(t, L) - \overline{w}_1(t, L)), \quad (40)$$

with boundary conditions,

$$\begin{pmatrix} \hat{w}_1(t, 0) \\ \hat{v}_2(t, 0) \\ \hat{v}_1(t, L) \\ \hat{w}_2(t, L) \end{pmatrix} = G \begin{pmatrix} \hat{w}_1(t, L) \\ \hat{v}_2(t, L) \\ \hat{v}_1(t, 0) \\ \hat{w}_2(t, 0) \end{pmatrix} + \begin{pmatrix} 0 \\ 0 \\ \frac{1 - r_1}{\rho_1^\star} \\ 0 \end{pmatrix} U_{\text{nom}}(t), \quad (41)$$

where G is given by (33). The terms μ_i and v_i are the output injection terms that are given as follows:

$$\mu_1(x) = v_1^\star N_1^{\alpha\alpha}(x, L), \quad v_1(x) = v_1^\star N_1^{\beta\alpha}(x, L), \quad (42)$$

$$\mu_2(x) = v_1^\star N^\alpha(x, L), \quad v_2(x) = v_1^\star N^\beta(x, L), \quad (43)$$

where the kernels $N_1^{\alpha\alpha}$, $N_1^{\beta\alpha}$, N^α, and N^β are bounded functions which are characterized in Appendix A.1.

3.2 | Emulation of the output-feedback control law

We aim at stabilizing the closed-loop system (28)–(32) on events while updating the continuous-time controller $U_{\text{nom}}(t)$ at certain sequence of time instants $(t_k)_{k\in\mathbb{N}}$, that will be characterized later on. The control value is held constant between two successive time instants and it is updated when some triggering condition is verified. This procedure is referred to as *event-triggering*. It is an efficient way to suitably apply (only when needed) the control value, thus avoiding useless actuation solicitations. To that end, we need to modify the control law proposed in Reference 20. More precisely, the control law $U_{\text{nom}}(t)$, that appears in (28)–(32) will be replaced by $U_{\text{nom}}(t_k)$ for all $t \in [t_k, t_{k+1})$, $k \geq 0$. It implies that the boundary conditions (32) and (41), become, respectively

$$
\begin{pmatrix} \overline{w}_1(t,0) \\ \overline{v}_2(t,0) \\ \overline{v}_1(t,L) \\ \overline{w}_2(t,L) \end{pmatrix} = G \begin{pmatrix} \overline{w}_1(t,L) \\ \overline{v}_2(t,L) \\ \overline{v}_1(t,0) \\ \overline{w}_2(t,0) \end{pmatrix} + \begin{pmatrix} 0 \\ 0 \\ \frac{1-r_1}{\rho_1^\star} \\ 0 \end{pmatrix} U_{\text{nom}}(t_k), \tag{44}
$$

and

$$
\begin{pmatrix} \hat{w}_1(t,0) \\ \hat{v}_2(t,0) \\ \hat{v}_1(t,L) \\ \hat{w}_2(t,L) \end{pmatrix} = G \begin{pmatrix} \hat{w}_1(t,L) \\ \hat{v}_2(t,L) \\ \hat{v}_1(t,0) \\ \hat{w}_2(t,0) \end{pmatrix} + \begin{pmatrix} 0 \\ 0 \\ \frac{1-r_1}{\rho_1^\star} \\ 0 \end{pmatrix} U_{\text{nom}}(t_k), \tag{45}
$$

for all $t \in [t_k, t_{k+1})$, where G is given by (33).

Consequently, we have $U_{\text{nom}}(t_k) = U_{\text{nom}}(t) + d(t)$, where d can be seen as a deviation of actuation. Since we need to assess the impact of the deviation $d(t)$ to the closed-loop system under the event-triggered implementation, we use some suitable backstepping transformations so that we can work on some target systems with desired stability properties (e.g., meeting Assumption 1) and that exhibit the deviation $d(t)$ at the boundary. From the target system, we can then perform an easier Lyapunov stability analysis while studying the event-triggered mechanism that we propose in the next section.

To that end, we define the error states a as the difference between the real states and their estimations: $\tilde{w}_i = \overline{w}_i - \hat{w}_i$ and $\tilde{v}_i = \overline{v}_i - \hat{v}_i$. The error system rewrites as

$$
\partial_t \tilde{w}_1(t,x) + v_1^\star \partial_x \tilde{w}_1(t,x) = \mu_1(x)\tilde{w}_1(t,L), \tag{46}
$$

$$
\partial_t \tilde{v}_2(t,x) + (\gamma_2 p_2^\star - v_2^\star)\partial_x \tilde{v}_2(t,x) = c_2(x)\tilde{w}_2(t,x) + v_2(x)\tilde{w}_1(t,L), \tag{47}
$$

$$
\partial_t \tilde{v}_1(t,x) - (\gamma_1 p_1^\star - v_1^\star)\partial_x \tilde{v}_1(t,x) = c_1(x)\tilde{w}_1(t,x) + v_1(x)\tilde{w}_1(t,L), \tag{48}
$$

$$
\partial_t \tilde{w}_2(t,x) - v_2^\star \partial_x \tilde{w}_2(t,x) = \mu_2(x)\tilde{w}_1(t,L), \tag{49}
$$

with boundary conditions,

$$
\begin{pmatrix} \tilde{w}_1(t,0) \\ \tilde{v}_2(t,0) \\ \tilde{v}_1(t,L) \\ \tilde{w}_2(t,L) \end{pmatrix} = G \begin{pmatrix} \tilde{w}_1(t,L) \\ \tilde{v}_2(t,L) \\ \tilde{v}_1(t,0) \\ \tilde{w}_2(t,0) \end{pmatrix}, \tag{50}
$$

where G is given by (33). Consider next the following backstepping transformation $\begin{pmatrix} \tilde{w}_1(t,x) \\ \tilde{v}_1(t,x) \\ \tilde{w}_2(t,x) \\ \tilde{v}_2(t,x) \end{pmatrix} = \left(\mathcal{N} \begin{pmatrix} \tilde{\alpha}_1(t,\cdot) \\ \tilde{\beta}_1(t,\cdot) \\ \tilde{\alpha}_2(t,\cdot) \\ \tilde{\beta}_2(t,\cdot) \end{pmatrix} \right)(x)$, which

is displayed as follows:

$$
\begin{pmatrix} \tilde{w}_1(t,x) \\ \tilde{v}_1(t,x) \\ \tilde{w}_2(t,x) \\ \tilde{v}_2(t,x) \end{pmatrix} = \begin{pmatrix} \tilde{\alpha}_1(t,x) \\ \tilde{\beta}_1(t,x) \\ \tilde{\alpha}_2(t,x) \\ \tilde{\beta}_2(t,x) \end{pmatrix} - \int_0^L \begin{pmatrix} N_1^{\alpha\alpha}(x,\xi)\mathbb{1}_{[x,L]}(\xi) & 0 & 0 & 0 \\ N_1^{\beta\alpha}(x,\xi)\mathbb{1}_{[x,L]}(\xi) & 0 & 0 & 0 \\ N_2^{\alpha}(x,\xi) & 0 & N_2^{\alpha\alpha}(x,\xi)\mathbb{1}_{[0,x]}(\xi) & 0 \\ N^{\beta}(x,\xi) & 0 & N_2^{\beta\alpha}(x,\xi)\mathbb{1}_{[0,x]}(\xi) & 0 \end{pmatrix} \begin{pmatrix} \tilde{\alpha}_1(t,\xi) \\ \tilde{\beta}_1(t,\xi) \\ \tilde{\alpha}_2(t,\xi) \\ \tilde{\beta}_2(t,\xi) \end{pmatrix} d\xi, \tag{51}
$$

where the different kernels are defined by (A1)–(A9) (in Appendix A.1). The transformation (51) is invertible. This can be seen by noticing first that the part acting on the states $\tilde{\alpha}_1$ and $\tilde{\beta}_1$ corresponds to a Volterra transformation (which is always invertible[60]). Then, the part acting on the states $\tilde{\alpha}_2$ and $\tilde{\beta}_2$ corresponds to a Volterra transformation to which is added an affine term that depends on $\tilde{\alpha}_1$ and $\tilde{\beta}_1$. This transformation, maps the error system (46)–(50) to the system

$$
\partial_t \tilde{\alpha}_1(t,x) + v_1^\star \partial_x \tilde{\alpha}_1(t,x) = 0, \tag{52}
$$

$$
\partial_t \tilde{\beta}_2(t,x) + (\gamma_2 p_2^\star - v_2^\star)\partial_x \tilde{\beta}_2(t,x) = 0, \tag{53}
$$

$$
\partial_t \tilde{\beta}_1(t,x) - (\gamma_1 p_1^\star - v_1^\star)\partial_x \tilde{\beta}_1(t,x) = 0, \tag{54}
$$

$$
\partial_t \tilde{\alpha}_2(t,x) - v_2^\star \partial_x \tilde{\alpha}_2(t,x) = 0 \tag{55}
$$

with boundary conditions,

$$
\begin{pmatrix} \tilde{\alpha}_1(t,0) \\ \tilde{\beta}_2(t,0) \\ \tilde{\beta}_1(t,L) \\ \tilde{\alpha}_2(t,L) \end{pmatrix} = G \begin{pmatrix} \tilde{\alpha}_1(t,L) \\ \tilde{\beta}_2(t,L) \\ \tilde{\beta}_1(t,0) \\ \tilde{\alpha}_2(t,0) \end{pmatrix}, \tag{56}
$$

where G is given by (33).

Remark 1. This target system is exponentially stable due to Assumption 1. It is worth saying that a Lyapunov-based characterization related to this assumption will be recalled in the next section since the event-triggered control design mainly relies on Lyapunov techniques.

In addition, the design of our event-triggered procedure requires the inverse transformation of (51). More precisely, we denote $\mathcal{R}$ the corresponding inverse transformation that is, $\begin{pmatrix} \tilde{\alpha}_1(t,x) \\ \tilde{\beta}_1(t,x) \\ \tilde{\alpha}_2(t,x) \\ \tilde{\beta}_2(t,x) \end{pmatrix} = \left(\mathcal{R} \begin{pmatrix} \tilde{w}_1(t,\cdot) \\ \tilde{v}_1(t,\cdot) \\ \tilde{w}_2(t,\cdot) \\ \tilde{v}_2(t,\cdot) \end{pmatrix} \right)(x)$ and which is displayed as follows:

$$
\begin{pmatrix} \tilde{\alpha}_1(t,x) \\ \tilde{\beta}_1(t,x) \\ \tilde{\alpha}_2(t,x) \\ \tilde{\beta}_2(t,x) \end{pmatrix} = \begin{pmatrix} \tilde{w}_1(t,x) \\ \tilde{v}_1(t,x) \\ \tilde{w}_2(t,x) \\ \tilde{v}_2(t,x) \end{pmatrix} - \int_0^L \begin{pmatrix} R_1^{ww}(x,\xi)\mathbb{1}_{[x,L]}(\xi) & 0 & 0 & 0 \\ R_1^{vw}(x,\xi)\mathbb{1}_{[x,L]}(\xi) & 0 & 0 & 0 \\ R^{w}(x,\xi) & 0 & R_2^{ww}(x,\xi)\mathbb{1}_{[0,x]}(\xi) & 0 \\ R^{v}(x,\xi) & 0 & R_2^{wv}(x,\xi)\mathbb{1}_{[0,x]}(\xi) & 0 \end{pmatrix} \begin{pmatrix} \tilde{w}_1(t,\xi) \\ \tilde{v}_1(t,\xi) \\ \tilde{w}_2(t,\xi) \\ \tilde{v}_2(t,\xi) \end{pmatrix} d\xi. \tag{57}
$$

The different kernels of (57) are bounded functions and are characterized in Appendix A.2.

Finally we use the backstepping transformation $\begin{pmatrix} \hat{\alpha}_1(t,x) \\ \hat{\beta}_1(t,x) \\ \hat{\alpha}_2(t,x) \\ \hat{\beta}_2(t,x) \end{pmatrix} = \left(\mathcal{K} \begin{pmatrix} \hat{w}_1(t,\cdot) \\ \hat{v}_1(t,\cdot) \\ \hat{w}_2(t,\cdot) \\ \hat{v}_2(t,\cdot) \end{pmatrix} \right)(x)$ which is displayed as follows:

$$
\begin{pmatrix} \hat{\alpha}_1(t,x) \\ \hat{\beta}_1(t,x) \\ \hat{\alpha}_2(t,x) \\ \hat{\beta}_2(t,x) \end{pmatrix} = \begin{pmatrix} \hat{w}_1(t,\cdot) \\ \hat{v}_1(t,\cdot) \\ \hat{w}_2(t,\cdot) \\ \hat{v}_2(t,\cdot) \end{pmatrix} - \int_0^L \begin{pmatrix} 0 & 0 & 0 & 0 \\ K_1^{vw}(x,\xi)\mathbb{1}_{[0,x]}(\xi) & K_1^{vv}(x,\xi)\mathbb{1}_{[0,x]}(\xi) & K^{w}(x,\xi) & K^{v}(x,\xi) \\ 0 & 0 & 0 & 0 \\ 0 & 0 & K_2^{vw}(x,\xi)\mathbb{1}_{[x,L]}(\xi) & K_2^{vv}(x,\xi)\mathbb{1}_{[x,L]}(\xi) \end{pmatrix} \begin{pmatrix} \hat{w}_1(t,\xi) \\ \hat{v}_1(t,\xi) \\ \hat{w}_2(t,\xi) \\ \hat{v}_2(t,\xi) \end{pmatrix} d\xi. \tag{58}
$$

This transformations maps the observer system (37)–(40), (45) into the following target system with a boundary disturbance term (the deviation $d(t)$):

$$\partial_t \hat{\alpha}_1(t,x) + v_1^\star \partial_x \hat{\alpha}_1(t,x) = p_{\mu_1}(x)\tilde{\alpha}_1(t,L), \tag{59}$$

$$\partial_t \hat{\beta}_2(t,x) + (\gamma_2 p_2^\star - v_2^\star)\partial_x \hat{\beta}_2(t,x) = p_{v_2}(x)\tilde{\alpha}_1(t,L), \tag{60}$$

$$\partial_t \hat{\beta}_1(t,x) - (\gamma_1 p_1^\star - v_1^\star)\partial_x \hat{\beta}_1(t,x) = p_{v_1}(x)\tilde{\alpha}_1(t,L), \tag{61}$$

$$\partial_t \hat{\alpha}_2(t,x) - v_2^\star \partial_x \hat{\alpha}_2(t,x) = p_{\mu_2}(x)\tilde{\alpha}_1(t,L), \tag{62}$$

with boundary conditions,

$$\begin{pmatrix} \hat{\alpha}_1(t,0) \\ \hat{\beta}_2(t,0) \\ \hat{\beta}_1(t,L) \\ \hat{\alpha}_2(t,L) \end{pmatrix} = G \begin{pmatrix} \hat{\alpha}_1(t,L) \\ \hat{\beta}_2(t,L) \\ \hat{\beta}_1(t,0) \\ \hat{\alpha}_2(t,0) \end{pmatrix} + \begin{pmatrix} 0 \\ 0 \\ \frac{1-r_1}{\rho_1^\star} \\ 0 \end{pmatrix} d(t), \tag{63}$$

where G is given by (33), and

$$p_{\mu_1}(x) = -\mu_1(x), \tag{64}$$

$$p_{v_1}(x) = -v_1(x) + \int_0^x K_1^{vw}(x,\xi)\mu_1(\xi) + K_1^{vv}(x,\xi)v_1(\xi)d\xi + \int_0^L K^w(x,\xi)\mu_2(\xi) + K^v(x,\xi)v_2(\xi)d\xi, \tag{65}$$

$$p_{\mu_2}(x) = -\mu_2(x), \tag{66}$$

$$p_{v_2}(x) = -v_2(x) + \int_x^L K_2^{vw}(x,\xi)\mu_2(\xi) + K_2^{vv}(x,\xi)v_2(\xi)d\xi, \tag{67}$$

Note that the functions p_{v_1} and p_{v_2} are well-defined since they are solutions of Volterra equations.[60]

The transformation (58) is invertible and the inverse transformation (which is a key in the design our event-triggered controller) is given by $\begin{pmatrix} \hat{w}_1(t,x) \\ \hat{v}_1(t,x) \\ \hat{w}_2(t,x) \\ \hat{v}_2(t,x) \end{pmatrix} = \mathcal{L}\left(\begin{pmatrix} \hat{\alpha}_1(t,\cdot) \\ \hat{\beta}_1(t,\cdot) \\ \hat{\alpha}_2(t,\cdot) \\ \hat{\beta}_2(t,\cdot) \end{pmatrix} \right)(x)$ and is displayed as follows:

$$\begin{pmatrix} \hat{w}_1(t,x) \\ \hat{v}_1(t,x) \\ \hat{w}_2(t,x) \\ \hat{v}_2(t,x) \end{pmatrix} = \begin{pmatrix} \hat{\alpha}_1(t,\cdot) \\ \hat{\beta}_1(t,\cdot) \\ \hat{\alpha}_2(t,\cdot) \\ \hat{\beta}_2(t,\cdot) \end{pmatrix} + \int_0^L \begin{pmatrix} 0 & 0 & 0 & 0 \\ L_1^{\beta\alpha}(x,\xi)\mathbb{1}_{[0,x]}(\xi) & L_1^{\beta\beta}(x,\xi)\mathbb{1}_{[0,x]}(\xi) & L^\alpha(x,\xi) & L^\beta(x,\xi) \\ 0 & 0 & 0 & 0 \\ 0 & 0 & L_2^{\beta\alpha}(x,\xi)\mathbb{1}_{[x,L]}(\xi) & L_2^{\beta\beta}(x,\xi)\mathbb{1}_{[x,L]}(\xi) \end{pmatrix} \begin{pmatrix} \hat{\alpha}_1(t,\xi) \\ \hat{\beta}_1(t,\xi) \\ \hat{\alpha}_2(t,\xi) \\ \hat{\beta}_2(t,\xi) \end{pmatrix} d\xi, \tag{68}$$

The different kernels of the transformation (68) are bounded functions and are characterized in Appendix A.4.

Using the inverse transformation (68), we can now rewrite the nominal control law U_{nom} defined by (36) as a function of the states $\hat{\alpha}_i$ and $\hat{\beta}_i$

$$U_{\text{nom}}(t) = \frac{\rho_1^\star}{1-r_1}\left(\int_0^L \left(L_1^{\beta\alpha}(L,\xi)\hat{\alpha}_1(t,\xi) + L_1^{\beta\beta}(L,\xi)\hat{\beta}_1(t,\xi) \right) d\xi + \int_0^L \left(L^\alpha(L,\xi)\hat{\alpha}_2(t,\xi) + L^\beta(L,\xi)\hat{\beta}_2(t,\xi) \right) d\xi \right), \tag{69}$$

and the corresponding emulated version

$$U_{\text{nom}}(t_k) = \frac{\rho_1^\star}{1-r_1}\left(\int_0^L \left(L_1^{\beta\alpha}(L,\xi)\hat{\alpha}_1(t_k,\xi) + L_1^{\beta\beta}(L,\xi)\hat{\beta}_1(t_k,\xi) \right) d\xi + \int_0^L \left(L^\alpha(L,\xi)\hat{\alpha}_2(t_k,\xi) + L^\beta(L,\xi)\hat{\beta}_2(t_k,\xi) \right) d\xi \right), \tag{70}$$

for all $t \in [t_k, t_{k+1})$. We recall that $U_{\text{nom}}(t_k) = U_{\text{nom}}(t) + d(t)$ where d is given by

$$
\begin{aligned}
d(t) = \frac{\rho_1^{\star}}{1 - r_1} \Bigg(& \int_0^L \left(L_1^{\beta\alpha}(L, \xi)(\hat{\alpha}_1(t_k, \xi) - \hat{\alpha}_1(t, \xi)) + L_1^{\beta\beta}(L, \xi)(\hat{\beta}_1(t_k, \xi) - \hat{\beta}_1(t, \xi)) \right) d\xi \\
& + \int_0^L \left(L^{\alpha}(L, \xi)(\hat{\alpha}_2(t_k, \xi) - \hat{\alpha}_2(t, \xi)) + L^{\beta}(L, \xi)(\hat{\beta}_2(t_k, \xi) - \hat{\beta}_2(t, \xi)) \right) d\xi \Bigg).
\end{aligned}
\tag{71}
$$

As aforementioned, the function d can be viewed as an actuation deviation between the continuous (nominal) controller and the event-triggered one. Notice that the nominal control, as well as its emulated version are expressed in terms of the kernels of transformation (68) and the states of the new target system (59)–(67). One of the main advantages of such an expression is that it can be easier to work with the target system (particularly when considering Lyapunov analysis and input-to-state stability ISS properties of the system with respect to the deviation d). It also allows an easier study of the *growth-in-time* of the deviation of actuation $d(t)$ (which is crucial to prove the avoidance of the so-called Zeno phenomenon). This is of specific interest when emulating the control law and finding conditions that guarantee the closed-loop stability under any event-triggered strategy. This methodology has been used in for example, References 36,37,50,61.

Before we proceed with the definition of the observer-based event-triggered control, we need to introduce several parameters that will be involved in the analysis and design.

Using the kernels of the transformation (68) (which are solutions to A33–A34) along with (64)–(67), we introduce the following variables:

$$
\kappa_{\hat{\alpha}_1} = 8 \left(\frac{\rho_1^{\star}}{1 - r_1} \right)^2 \left(v_1^{\star} L_1^{\beta\alpha}(L, L) + v_1^{\star} \exp\left(\frac{-L}{\tau_1 v_1^{\star}} \right) L_1^{\beta\beta}(L, L) \right)^2,
\tag{72}
$$

$$
\kappa_{\hat{\beta}_1} = 8 \left(\frac{\rho_1^{\star}}{1 - r_1} \right)^2 \left((\gamma_1 p_1^{\star} - v_1^{\star}) L_1^{\beta\beta}(L, 0) + \delta \frac{v_2^{\star}}{r_1} L^{\beta}(L, 0) \right)^2,
\tag{73}
$$

$$
\kappa_{\hat{\alpha}_2} = 8 \left(\frac{\rho_1^{\star}}{1 - r_1} \right)^2 \left(-v_1^{\star} L_1^{\beta\alpha}(L, 0) + v_2^{\star} L^{\alpha}(L, 0) + (1 - \delta) v_2^{\star} L^{\beta}(L, 0) \right)^2,
\tag{74}
$$

$$
\kappa_{\hat{\beta}_2} = 8 \left(\frac{\rho_1^{\star}}{1 - r_1} \right)^2 \left(-v_2^{\star} \frac{1}{r_2} \exp\left(\frac{-L}{\tau_2 v_2^{\star}} \right) L^{\alpha}(L, L) + (\gamma_2 p_2^{\star} - v_2^{\star}) L^{\beta}(L, L) \right)^2,
\tag{75}
$$

$$
\kappa_{\tilde{\alpha}_1} = 4 \left(\frac{\rho_1^{\star}}{1 - r_1} \right)^2 \left(\int_0^L \left(L_1^{\beta\alpha}(L, \xi) p_{\mu_1}(\xi) + L_1^{\beta\beta}(L, \xi) p_{v_1}(\xi) + L^{\alpha}(L, \xi) p_{\mu_2}(\xi) + L^{\beta}(L, \xi) p_{v_2}(\xi) \right) d\xi \right)^2,
\tag{76}
$$

$$
\begin{aligned}
\varepsilon_0 = 2 \left(\frac{\rho_1^{\star}}{1 - r_1} \right)^2 \max \Bigg\{ & \int_0^L \left(v_1^{\star} \partial_{\xi} L_1^{\beta\alpha}(L, \xi) \right)^2 d\xi, \\
& \int_0^L \left((\gamma_1 p_1^{\star} - v_1^{\star}) \partial_{\xi} L_1^{\beta\beta}(L, \xi) \right)^2 d\xi, \\
& \int_0^L \left(v_2^{\star} \partial_{\xi} L^{\alpha}(L, \xi) \right)^2 d\xi, \int_0^L \left((\gamma_2 p_2^{\star} - v_2^{\star}) \partial_{\xi} L^{\beta}(L, \xi) \right)^2 d\xi \Bigg\},
\end{aligned}
\tag{77}
$$

$$
\varepsilon_1 = 4 \left((\gamma_1 p_1^{\star} - v_1^{\star}) L_1^{\beta\beta}(L, L) \right)^2.
\tag{78}
$$

In particular, these variables come into play in the triggering condition and in the study of the Zeno phenomenon. Notice that they depend only on the traffic parameters and the gains of the boundary controller.

4 | OBSERVER-BASED EVENT-TRIGGERED BOUNDARY CONTROL STRATEGY

In this section we study the observer-based event-triggered boundary control strategy proposed in this article. It encloses an event-trigger mechanism containing a suitable triggering condition (which determines the time instant at which the controller needs to be updated) and the output feedback controller (70).

The event-triggering condition is based on the evolution of the square of the actuation deviation (71) and of a dynamic variable satisfying a suitable ODE. More importantly, the triggering condition relies on a Lyapunov function for the target systems (52)–(56) and (59)–(63).

4.1 | Lyapunov-based characterization towards the definition of the triggering condition

At this stage, it is important to bring back and highlight condition of Assumption 1 and its relation with a Lyapunov-based characterization. To see this, consider first the target system (52)–(56) for which we can recall the following result:

Proposition 1. *If the dissipative condition (35) in Assumption 1 is satisfied, then the system (52)–(56) is exponentially stable.*

A rigorous proof can be found in for example, Reference 56 or in Reference 9 (section 3). It is important, however, to recall some important elements: A Lyapunov function candidate is defined for all $(\tilde{\alpha}_i(t, \cdot), \tilde{\beta}_i(t, \cdot)) \in L^2((0, L); \mathbb{R}^4)$ as follows:

$$V_1 = \int_0^L \begin{pmatrix} \tilde{\alpha}_1(t, x) \\ \tilde{\beta}_2(t, x) \end{pmatrix}^\top (\Lambda^+)^{-1} Q^+(\mu x) \begin{pmatrix} \tilde{\alpha}_1(t, x) \\ \tilde{\beta}_2(t, x) \end{pmatrix} dx + \int_0^L \begin{pmatrix} \tilde{\beta}_1(t, x) \\ \tilde{\alpha}_2(t, x) \end{pmatrix}^\top (\Lambda^-)^{-1} Q^-(\mu x) \begin{pmatrix} \tilde{\beta}_1(t, x) \\ \tilde{\alpha}_2(t, x) \end{pmatrix} dx, \tag{79}$$

with

$$\Lambda^+ = \text{diag} \left[v_1^\star, (\gamma_2 p_2^\star - v_2^\star) \right], \quad \Lambda^- = \text{diag} \left[(\gamma_1 p_1^\star - v_1^\star), v_2^\star \right], \tag{80}$$

and

$$Q^+(\mu x) = \text{diag} \left[\varrho_1^+ \exp\left(-\frac{\mu x}{v_1^\star} \right), \varrho_2^+ \exp\left(-\frac{\mu x}{\gamma_2 p_2^\star - v_2^\star} \right) \right], \quad \varrho_i^+ > 0,$$

$$Q^-(\mu x) = \text{diag} \left[\varrho_1^- \exp\left(\frac{\mu x}{\gamma_1 p_1^\star - v_1^\star} \right), \varrho_2^- \exp\left(\frac{\mu x}{v_2^\star} \right) \right], \quad \varrho_i^- > 0. \tag{81}$$

Under Assumption 1, it can be proved that one can find $\varrho_i^+, \varrho_i^- > 0$, $\mu > 0$ such that $\dot{V}_1$ is a negative definite function. Indeed, as long as there exists $\Delta = \text{diag}[\Delta_0, \Delta_1] \in \mathcal{D}_4^+$ such that $\|\Delta G \Delta^{-1}\| < 1$, one can take $Q^+(0) = \Delta_0^2$ and $Q^-(0) = \Delta_1^2$ hence finding ϱ_i^+ and $\varrho_i^- > 0^\dagger$. The existence of $\mu > 0$ sufficiently small follows by continuity arguments.

It is important to point out that, due to the structure of system (52)–(56) where G is given by (33), we can establish the following more conservative sufficient conditions for exponential stability and we can even explicitly characterize ϱ_i^+, $\varrho_i^- > 0$. The underlying conditions are the following:

$$\varrho_1^- \exp\left(\frac{\mu L}{\gamma_1 p_1^\star - v_1^\star} \right) \left(r_1 \exp\left(\frac{-L}{\tau_1 v_1^\star} \right) \right)^2 - \varrho_1^+ \exp\left(\frac{-\mu L}{v_1^\star} \right) < 0, \tag{82}$$

$$\varrho_2^- \exp\left(\frac{\mu L}{v_2^\star} \right) \left(\frac{1}{r_2} \exp\left(\frac{-L}{\tau_2 v_2^\star} \right) \right)^2 - \varrho_2^+ \exp\left(\frac{-\mu L}{\gamma_2 p_2^\star - v_2^\star} \right) < 0, \tag{83}$$

$$2 \left(\delta \frac{r_2}{r_1} \right)^2 \varrho_2^+ - \varrho_1^- < 0, \tag{84}$$

$$2((1 - \delta) r_2)^2 \varrho_2^+ + \varrho_1^+ - \varrho_2^- < 0. \tag{85}$$

For μ sufficiently small, we can explicitly set ϱ_i^+, ϱ_i^- (among many other possibilities) as follows:

$$\varrho_1^+ = \exp\left(\frac{\mu L}{v_1^\star} \right), \tag{86}$$

$$\varrho_2^+ = \exp\left(\frac{\mu L}{\gamma_2 p_2^\star - v_2^\star} \right), \tag{87}$$

$$\varrho_2^- = \frac{\left((1-\delta)^2 r_2^2\right)\exp\left(\frac{\mu L}{\gamma_2 p_2^\star - v_2^\star}\right) + \exp\left(\frac{\mu L}{v_1^\star}\right)}{2} + \frac{r_2^2}{2}\exp\left(\frac{-\mu L}{v_2^\star}\right)\exp\left(\frac{2L}{\tau_2 v_2^\star}\right), \tag{88}$$

$$\varrho_1^- = \varrho_2^-\left(\frac{1}{r_1 r_2}\right)^2\exp\left(\frac{2L}{\tau_1 v_1^\star} - \frac{2L}{\tau_2 v_2^\star} - \frac{\mu L}{\gamma_1 p_1^\star - v_1^\star} + \frac{\mu L}{v_2^\star}\right). \tag{89}$$

In addition, we define similarly a Lyapunov function for the target system (59)–(63).

$$V_2 = \int_0^L \begin{pmatrix}\hat{\alpha}_1(t,x)\\\hat{\beta}_2(t,x)\end{pmatrix}^\top (\Lambda^+)^{-1}Q^+(\mu x)\begin{pmatrix}\hat{\alpha}_1(t,x)\\\hat{\beta}_2(t,x)\end{pmatrix}dx + \int_0^L \begin{pmatrix}\hat{\beta}_1(t,x)\\\hat{\alpha}_2(t,x)\end{pmatrix}^\top (\Lambda^-)^{-1}Q^-(\mu x)\begin{pmatrix}\hat{\beta}_1(t,x)\\\hat{\alpha}_2(t,x)\end{pmatrix}dx, \tag{90}$$

where, as before, $Q^+(\mu x)$, $Q^-(\mu x)$ are given in (81) along with the explicit characterization of ϱ_i^+, ϱ_i^- given in (86)–(88) and μ sufficiently small. In addition, it is worth recalling that there exist $\underline{\varpi}_2$, $\overline{\varpi}_2$ (depending on ϱ_i^+, ϱ_i^- and on μ) such that $\underline{\varpi}_2\|(\hat{\alpha}_i(t,\cdot),\hat{\beta}_i(t,\cdot))\|_{L^2}^2 \leq V_2 \leq \overline{\varpi}_2\|(\hat{\alpha}_i(t,\cdot),\hat{\beta}_i(t,\cdot))\|_{L^2}^2, i = 1, 2$. Thus, V_2 is equivalent to the L^2-norm. In particular, $\underline{\varpi}_2$ can be derived explicitly as follows:

$$\underline{\varpi}_2 = \min\left\{\frac{1}{v_1^\star}, \frac{1}{\gamma_2 p_2^\star - v_2^\star}, \frac{\varrho_1^-}{\gamma_1 p_1^\star - v_1^\star}, \frac{\varrho_2^-}{v_2^\star}\right\}, \tag{91}$$

where ϱ_2^- and ϱ_1^- are respectively given by (88) and (89).

Hence, we now can define the Lyapunov function that we are going to use in the triggering condition;

$$V = V_1 + CV_2, \tag{92}$$

where V_1, V_2 are respectively given by (79) and (90) with C being defined as follows:

$$C = \frac{\theta_0 \mu}{4 C_0}, \tag{93}$$

with

$$C_0 = \int_0^L \begin{pmatrix}p_{\mu_1}(x)\\p_{v_2}(x)\end{pmatrix}^\top (\Lambda^+)^{-1}Q^+(\mu x)\begin{pmatrix}p_{\mu_1}(x)\\p_{v_2}(x)\end{pmatrix}dx + \int_0^L \begin{pmatrix}p_{v_1}(x)\\p_{\mu_2}(x)\end{pmatrix}^\top (\Lambda^-)^{-1}Q^-(\mu x)\begin{pmatrix}p_{v_1}(x)\\p_{\mu_2}(x)\end{pmatrix}dx, \tag{94}$$

with some $\theta_0 > 0$ sufficiently small and where $p_{\mu_1}, p_{v_2}, p_{v_1}, p_{\mu_2}$ (output injection terms after transformation) are given in (64)–(67).

4.2 | Definition of observer-based event-triggered boundary controller

We are in position to define the observer-based event-triggered boundary controller.

Definition 1 (observer-based event-triggered boundary controller). Let $\kappa_{\hat{\alpha}_1}, \kappa_{\hat{\beta}_2}, \kappa_{\hat{\beta}_1}, \kappa_{\hat{\alpha}_2}, \kappa_{\tilde{\alpha}_1}$ be the parameters introduced in (72)–(76) (related to traffic modeling and boundary control gains). Let $V(t)$ the Lyapunov function be defined in (92) with $Q^+(\mu x)$, $Q^-(\mu x)$ be given in (81) along with the explicit characterization of ϱ_i^+, ϱ_i^- given in (86)–(88). Let $\mu > 0$, $\theta_0 > 0$ (sufficiently small), $\sigma \in (0,1)$ and $\theta_2 > 0$ be design parameters. Define

$$\theta_1 = 2\frac{\theta_0 \mu}{4 C_0}\left(\frac{1-r_1}{\rho_1^\star}\right)^2 \varrho_1^- \exp\left(\frac{\mu L}{\gamma_1 p_1^\star - v_1^\star}\right), \tag{95}$$

with C_0 given by (94).

The observer-based event-triggered boundary control is defined by considering the following components: (I) (The event-triggering condition) The times of the events $t_k \geq 0$ with $t_0 = 0$ form a finite or countable set of times which is determined by the following rules for some $k \geq 0$:

- if $\left\{ t \in \mathbb{R}^+ | t > t_k; \theta_1 d^2(t) \geq \frac{\mu}{2}\sigma V(t) - \frac{1}{\theta_2}m(t) \right\} = \emptyset$ then the set of the times of the events is $\{t_0, \ldots, t_k\}$.

- if $\left\{ t \in \mathbb{R}^+ | t > t_k; \theta_1 d^2(t) \geq \frac{\mu}{2}\sigma V(t) - \frac{1}{\theta_2}m(t) \right\} \neq \emptyset$, then the next event time is given by:

$$t_{k+1} = \inf \left\{ t \in \mathbb{R}^+ | t > t_k; \theta_1 d^2(t) \geq \frac{\mu}{2}\sigma V(t) - \frac{1}{\theta_2}m(t) \right\}, \tag{96}$$

where the actuation deviation $d(t)$ is given by (71) for all $t \in [t_k, t_{k+1})$, and m satisfies the ordinary differential equation,

$$\dot{m}(t) = -\mu(1-\sigma)m(t) + \theta_1 d^2(t) - \frac{\mu}{2}\sigma V(t) - 2\theta_1\theta_2 \left(\kappa_{\hat{\alpha}_1}\hat{\alpha}_1^2(t,L) + \kappa_{\hat{\beta}_2}\hat{\beta}_2^2(t,L) + \kappa_{\hat{\beta}_1}\hat{\beta}_1^2(t,0) + \kappa_{\hat{\alpha}_2}\hat{\alpha}_2^2(t,0) + \kappa_{\tilde{\alpha}_1}\tilde{\alpha}_1^2(t,L) \right), \tag{97}$$

for all $t \in (t_k, t_{k+1})$ with $m(0) = m^0 < 0$, and $m(t_k^-) = m(t_k) = m(t_k^+)$.

(II) (the control action) The output boundary feedback law is defined by

$$U_{\text{nom}}(t_k) = \frac{\rho_1^\star}{1 - r_1} \left(\int_0^L \left(L_1^{\beta\alpha}(L,\xi)\hat{\alpha}_1(t_k,\xi) + L_1^{\beta\beta}(L,\xi)\hat{\beta}_1(t_k,\xi) \right) d\xi + \int_0^L \left(L^\alpha(L,\xi)\hat{\alpha}_2(t_k,\xi) + L^\beta(L,\xi)\hat{\beta}_2(t_k,\xi) \right) d\xi \right), \tag{98}$$

for all $t \in [t_k, t_{k+1})$.

Remark 2. Although the function $V(t)$ (defined in 92 and involved in the triggering condition) depends on $\tilde{\alpha}_i(t,\cdot)$ and $\tilde{\beta}_i(t,\cdot)$ (which are a priori unknown), this is not a problem as these functions can be expressed as delayed functions of the measurement $Y_L(t)$ and of the observer state. Indeed, we have $\tilde{\alpha}(t,L) = \tilde{w}(t,L) = Y_L(t) - \hat{w}(t,L)$, which means that the function $\tilde{\alpha}(t,L)$ can be computed from the measurement. From (52)–(56), we immediately have for all $x \in [0,L]$

$$\tilde{\beta}_1(t,x) = r_1 \exp\left(\frac{-L}{\tau_1 v_1^\star}\right) \tilde{\alpha}_1 \left(t - \frac{L-x}{\gamma_1 p_1^\star - v_1^\star}, L \right), \tag{99}$$

which means that we can also compute the function $\tilde{\beta}_1(t,x)$ from the measurement. Consider now the function $\tilde{\alpha}_2(t,0)$. We have (using the method of characteristics)

$$\tilde{\alpha}_2(t,0) = \exp\left(\frac{-L}{\tau_2 v_2^\star}\right)(1-\delta)\tilde{\alpha}_2 \left(t - \frac{1}{v_2^\star} - \frac{1}{\gamma_2 p_2^\star - v_2^\star}, 0 \right) + \frac{\delta}{r_1} \exp\left(\frac{-L}{\tau_2 v_2^\star}\right) \tilde{\beta}_1 \left(t - \frac{1}{v_2^\star} - \frac{1}{\gamma_1 p_1^\star - v_1^\star}, 0 \right). \tag{100}$$

Applying the method of characteristics on the term $\tilde{\alpha}_2(\cdot, 0)$ that appears on the right side of the above equation, and iterating N_0 times the procedure (where N_0 is an integer), we obtain

$$\tilde{\alpha}_2(t,0) = \left(\exp\left(\frac{-L}{\tau_2 v_2^\star}\right)(1-\delta) \right)^{N_0} \tilde{\alpha}_2 \left(t - \left(\frac{1}{v_2^\star} + \frac{1}{\gamma_2 p_2^\star - v_2^\star} \right) N_0, 0 \right) + F(\tilde{\beta}_1(t,0)), \tag{101}$$

where the function F only depends on delayed values of $F(\tilde{\beta}_1(t,0))$. Choosing N_0 such that $\left(\frac{1}{v_2^\star} + \frac{1}{\gamma_2 p_2^\star - v_2^\star} \right) N_0 - \frac{1}{v_1^\star} > 0$ and using Equation (56), we obtain

$$\tilde{\alpha}_2(t,0) = \left(\exp\left(\frac{-L}{\tau_2 v_2^\star}\right)(1-\delta) \right)^{N_0} \tilde{\alpha}_1 \left(t - \left(\frac{1}{v_2^\star} + \frac{1}{\gamma_2 p_2^\star - v_2^\star} \right) N_0 + \frac{1}{v_1^\star}, L \right) + F(\tilde{\beta}_1(t,0)). \tag{102}$$

Thus, we can compute the function $\tilde{\alpha}_2(t,0)$ using the available measurement. Using the method of the characteristics, it becomes straightforward to express $\tilde{\alpha}_i(t,x)$ and $\tilde{\beta}_i(t,x)$ as delayed functions of the available measurements. Thus, the proposed event-triggered strategy is implementable.

Remark 3. We have introduced numerous parameters related to the traffic modeling, control gains, and new design parameters related to the triggering condition. For the sake of clarity, we distinguish and summarize some of them in

Table 1. Among the parameters, let us point out some important aspects of those involved in the triggering condition. For instance, σ and θ_2 are instrumental in adjusting the sampling speed. The smaller σ, the faster the sampling is. In addition, θ_2 is a key parameter that makes the dynamic variable $m(t)$ to come into play. It is worth saying that dynamic triggering conditions have been useful to reduce the number of execution times relative to static triggering conditions and hence obtaining larger inter-execution times; see for instance Reference 44 in the framework of finite-dimensional systems and Reference 30 for infinite-dimensional systems. Here, the smaller θ_2, the more influence the dynamic variable has. The larger θ_2 or even when θ_2 goes to $+\infty$, one ends up dealing with a *static* event-triggering condition. Nevertheless, this limiting case is not studied in this article since, under a static triggering condition with boundary control for this class of PDE system, the existence of a minimal dwell-time (and hence the avoidance of the Zeno phenomenon) may not be easily derived (see Reference 36 for further discussion).

We directly have the following lemma.

Lemma 1. *Under the definition of the observer-based event triggered boundary control (98) with the dynamic triggering condition (96), it holds that $\theta_1 d^2(t) - \frac{\mu}{2}\sigma V(t) + \frac{1}{\theta_2}m(t) < 0$ and $m(t) < 0$ for $t \in [0, T)$ where $T = \lim_{k\to\infty}(t_k)$.*

Proof. From the definition of the dynamic triggering condition (96)–(97), events are triggered to guarantee $\theta_1 d^2(t) - \frac{\mu}{2}\sigma V(t) + \frac{1}{\theta_2}m(t) < 0$, for $t \in [t_k, t_{k+1})$. This inequality in conjunction with (97) yields,

$$\dot{m}(t) \leq -\left(\mu(1-\sigma) + \frac{1}{\theta_2}\right)m(t) - 2\theta_1\theta_2\left(\kappa_{\hat{\alpha}_1}\hat{\alpha}_1^2(t,L) + \kappa_{\hat{\beta}_2}\hat{\beta}_2^2(t,L) + \kappa_{\hat{\beta}_1}\hat{\beta}_1^2(t,0) + \kappa_{\hat{\alpha}_2}\hat{\alpha}_2^2(t,0) + \kappa_{\tilde{\alpha}_1}\tilde{\alpha}_1^2(t,L)\right), \tag{103}$$

for $t \in (t_k, t_{k+1})$. Due to the continuity of $m(t)$, we can obtain the following estimate:

$$m(t) \leq \exp\left(-\left(\mu(1-\sigma) + \frac{1}{\theta_2}\right)(t - t_k)\right)m(t_k) - 2\theta_1\theta_2\int_{t_k}^t \exp\left(-\left(\mu(1-\sigma) + \frac{1}{\theta_2}\right)(t - s)\right)\left(\kappa_{\hat{\alpha}_1}\hat{\alpha}_1^2(s,L)\right.$$
$$\left. + \kappa_{\hat{\beta}_2}\hat{\beta}_2^2(s,L) + \kappa_{\hat{\beta}_1}\hat{\beta}_1^2(s,0) + \kappa_{\hat{\alpha}_2}\hat{\alpha}_2^2(s,0) + \kappa_{\tilde{\alpha}_1}\tilde{\alpha}_1^2(s,L)\right)ds, \tag{104}$$

for $t \in [t_k, t_{k+1}]$. Since $m(t_0) < 0$ (from Definition 1), then it holds $m(t) < 0$ for all $t \in [0, t_1]$. Using (104) on $[t_1, t_2]$, we can show that $m(t) < 0$ for all $t \in [t_1, t_2]$. Applying the same reasoning successively to the future intervals, we can deduce that $m(t) < 0$ for all $t \in [0, T)$. This concludes the proof. ■

The following result is useful to analyze the growth-in-time of the actuation deviation. A suitable characterization is given in the following lemma which is instrumental to derive the existence of a minimal dwell-time.

Lemma 2. *For $d(t)$ given by (71), it holds for all $t \in (t_k, t_{k+1})$,*

$$(\dot{d}(t))^2 \leq \varepsilon_0 \frac{1}{\underline{\varpi}_2 C}V(t) + \varepsilon_1 d^2(t) + \kappa_{\hat{\alpha}_1}\hat{\alpha}_1^2(t,L) + \kappa_{\hat{\beta}_2}\hat{\beta}_2^2(t,L) + \kappa_{\hat{\beta}_1}\hat{\beta}_1^2(t,0) + \kappa_{\hat{\alpha}_2}\hat{\alpha}_2^2(t,0) + \kappa_{\tilde{\alpha}_1}\tilde{\alpha}_1^2(t,L), \tag{105}$$

where $\kappa_{\hat{\alpha}_1}$, $\kappa_{\hat{\beta}_2}$, $\kappa_{\hat{\beta}_1}$, $\kappa_{\hat{\alpha}_2}$, $\kappa_{\tilde{\alpha}_1}$, ε_0, ε_1 are given by (72)–(78), and $\underline{\varpi}_2$ and C are given, respectively, by (91) and (93).

Proof. The proof follows the same lines of Reference 36 lemma 2. ■

5 | MAIN RESULTS

In this section we present our main results: the avoidance of the Zeno phenomenon and the exponential convergence in L^2-norm of the closed-loop system.

5.1 | Avoidance of the Zeno phenomenon

We first prove the avoidance of the Zeno phenomenon.

TABLE 1   Traffic and observer-based event-triggered boundary control parameters

Category	Symbol	Description
Traffic parameters	$\rho_{m,i}$	Max. traffic densities
	v_m	Maximum traffic velocity
	$p_i^\star$	Traffic pressure coefficients
	γ_i	Overall drivers' behavior to the increase of density
	τ_i	Relaxation times
	$\rho_i^\star, v_i^\star$	Congested (density, velocity) steady states
	$q^\star$	Steady state flow
	r_i	Ratio of the characteristic speeds of the segments
	δ	Ratio of the traffic pressure
	L	Road segment length
Control gain parameter	$L_1^{\beta\alpha}(L,\cdot),\, L_1^{\beta\beta}(L,\cdot),\, L^\alpha(L,\cdot),\, L^\beta(L,\cdot)$	Kernel control gains
	$\kappa_{\hat{\alpha}_1},\, \kappa_{\hat{\beta}_2},\, \kappa_{\hat{\beta}_1},\, \kappa_{\hat{\alpha}_2},\, \kappa_{\hat{\alpha}_1},\, \varepsilon_0,\, \varepsilon_1$	Related to the growth-in-time of the deviation of actuation and involved in the dynamic triggering condition
Event-triggering condition	$\theta_0, \theta_1, \theta_2$	Involved in the dynamic triggering condition
	μ, σ	Decay rate
	ϱ_i^+, ϱ_i^-	Related parameters. Lyapunov related and involved in the dynamic triggering condition
	C	parameters

Theorem 1. *Under the event-triggered boundary control (98)–(96) in Definition 1, with parameters satisfying*

$$\frac{8\left(\frac{1-r_1}{\rho_1^\star}\right)^2 \varrho_1^- \exp\left(\frac{\mu L}{\gamma_1 p_1^\star - v_1^\star}\right) \varepsilon_0}{\min\left\{\frac{1}{v_1^\star}, \frac{1}{\gamma_2 p_2^\star - v_2^\star}, \frac{\varrho_1^-}{\gamma_1 p_1^\star - v_1^\star}, \frac{\varrho_2^-}{v_2^\star}\right\}} < \frac{\mu\sigma}{\theta_2}, \tag{106}$$

there exists a minimal dwell-time $\tau^\star > 0$ between two triggering times, that is, there exists a constant $\tau^\star > 0$ (independent of the initial conditions) such that $t_{k+1} - t_k \geq \tau^\star$, for all $k \geq 0$.

Remark 4. As we will see, condition (106) is a requirement to be able to derive a minimal dwell-time. Notice that on the left-hand side of inequality (106) most of the parameters are related to the traffic modeling and kernel control gain whereas on the right-hand side we have the parameters related to the triggering condition (see Table 1 for convenience). This condition gives some preliminary suggestions on how to suitable select the parameters involved in the triggering condition according to some constraints imposed by the traffic problem modeling and the kernel control gain. While μ is sufficiently small as discussed in Section 4.1, the resulting term on the left-hand-side may still turn out to be large. For example ϱ_1^- (see 88 and 89) may turn out to be large due to some terms such as $\exp\left(\frac{2L}{\tau_2 v_2^\star}\right)$ in (88) with the velocity $v_2^\star$ being very small relative to the length of the road L, or due to the term $\left(\frac{1}{r_1 r_2}\right)^2$ in (89) being large when the traffic is more congested. Besides, ε_0 (given in 77) which is a parameter related to the kernel control gain, may also be large whenever the spatial-variation of the control gain is significant (e.g., in cases when the stop-and-go oscillation phenomenon is substantial). Consequently, one would have to select σ or θ_2 small enough so that this condition can always be verified. If θ_2 is selected sufficiently small, the dynamic variable plays a more important role while triggering.

Proof. We adapt the methodology employed in References 36 and 37 to our observer-based event-triggered controller. From the definition of the event-triggered mechanism given in Definition 1, events are triggered when the condition $\theta_1 d^2(t) \geq \frac{\mu}{2}\sigma V(t) - \frac{1}{\theta_2}m(t)$ is satisfied. Based on this condition, we define the function

$$\psi(t) = \frac{\theta_1\theta_2 d^2(t) + \frac{1}{2}m(t)}{-12m(t) + \theta_2\mu 2\sigma V}, \tag{107}$$

which is continuous on $[t_k, t_{k+1})$. Consider now a more conservative event-triggering condition, for example, $\theta_1 d^2(t) \geq -\frac{1}{\theta_2}m(t)$ that enforces the events to occur faster. Therefore, let us define the function

$$\psi^\star(t) = \frac{\theta_1\theta_2 d^2(t) + \frac{1}{2}m(t)}{-12m(t)}, \tag{108}$$

which is continuous on $[t_k, t_{k+1}^\star)$ where $t_{k+1}^\star < t_{k+1}$. A lower bound for the inter-execution times is given by the time it takes for the function ψ to go from $\psi(t_k)$ to $\psi\left(t_{k+1}^-\right) = 1$, where $\psi(t_k) < 0$ which holds since $d(t_k) = 0$ ($m(t_k) < 0$ by virtue of Lemma 1). Here t_{k+1}^- is the left limit at $t = t_{k+1}$. Such a lower bound can further be lower bounded by the required time for the function $\psi^\star$ to go from $\psi^\star(t_k)$ to $\psi\left(t_{k+1}^{\star-}\right) = 1$, where $t_{k+1}^{\star-} < t_{k+1}^-$. Moreover, by the intermediate value theorem, there exists a $t_k' > t_k$ such that $\psi\left(t_k'\right) = \psi^\star\left(t_k'\right) = 0, \psi(t) \in [0, 1]$ for $t \in \left[t_k', t_{k+1}^-\right]$ and $\psi^\star(t) \in [0, 1]$ for $t \in \left[t_k', t_{k+1}^{\star-}\right]$. Notice that $\psi(t) < \psi^\star(t)$ for all $t \in \left[t_k', t_{k+1}^{\star-}\right]$. It is then sufficient to study the growth-in-time of $\psi^\star(t)$ on $t \in \left[t_k', t_{k+1}^{\star-}\right]$. The time derivative of $\psi^\star$ on $\left[t_k', t_{k+1}^\star\right)$ is given by

$$\dot{\psi}^\star(t) = \frac{2\theta_1\theta_2 d(t)\dot{d}(t) + \frac{1}{2}\dot{m}(t)}{-12m(t)} - \frac{\dot{m}(t)}{m(t)}\psi^\star(t). \tag{109}$$

Using the Young's inequality,

$$\dot{\psi}^\star(t) \leq \frac{\theta_1\theta_2 d^2(t) + \theta_1\theta_2 \dot{d}^2(t) + \frac{1}{2}\dot{m}(t)}{-12m(t)} - \frac{\dot{m}(t)}{m(t)}\psi^\star(t). \tag{110}$$

Then, using (97) along with (105) and reorganizing terms, we obtain the following estimate:

$$\dot{\psi}^{\star}(t) \leq \frac{\theta_1\theta_2 d^2(t)\left(1 + \varepsilon_1 + \frac{1}{2\theta_2}\right)}{-12m(t)} + \frac{V(t)\left(\theta_1\theta_2\frac{1}{\underline{\varpi}_2}\varepsilon_0 - \frac{\mu}{4}\sigma\right)}{-12m(t)} + \mu(1-\sigma) + \mu(1-\sigma)\psi^{\star}(t) - \frac{\theta_1 d^2(t)}{m(t)}\psi^{\star}(t)$$

$$+ \frac{\frac{\mu}{2}\sigma V(t)}{m(t)}\psi^{\star}(t) + 2\theta_1\theta_2\frac{\kappa_{\hat{\alpha}_1}\hat{\alpha}_1^2(t,L) + \kappa_{\hat{\beta}_2}\hat{\beta}_2^2(t,L) + \kappa_{\hat{\beta}_1}\hat{\beta}_1^2(t,0)}{m(t)}\psi^{\star}(t) + 2\theta_1\theta_2\frac{\kappa_{\hat{\alpha}_2}\hat{\alpha}_2^2(t,0) + \kappa_{\tilde{\alpha}_1}\tilde{\alpha}_1^2(t,L)}{m(t)}\psi^{\star}(t). \quad (111)$$

In light of condition (106), we have that the term $\theta_1\theta_2\frac{1}{\underline{\varpi}_2}\varepsilon_0 - \frac{\mu}{4}\sigma < 0$ (notice that the involved parameters ε_0, $\underline{\varpi}_2$, θ_1, are given in 77,91, and 95, respectively). In addition, using the definition of $\psi^{\star}$ in (108) and noticing that the last three terms in (111) are negative, we obtain the following differential inequality:

$$\dot{\psi}^{\star}(t) \leq a_0 + a_1\psi^{\star}(t) + a_2\psi^{\star 2}(t), \quad (112)$$

where

$$a_0 = 1 + \varepsilon_1 + \frac{1}{2\theta_2} + \mu(1-\sigma),$$

$$a_1 = 1 + \varepsilon_1 + \frac{1}{2\theta_2} + \mu(1-\sigma),$$

$$a_2 = \frac{1}{2\theta_2}.$$

The coefficients a_0, a_1, and a_2 are positive scalars (recall that ε_1 is a parameter related to the control gain as given in 78 whereas μ, θ_2, $\sigma \in (0,1)$ are design parameters involved in the triggering condition; thus influence the duration of the inter-sampling time). Hence, by the comparison principle, it follows that the time needed by $\psi^{\star}$ to go from $\psi^{\star}\left(t_k'\right) = 0$ to $\psi\left(t_{k+1}^{\star-}\right) = 1$ is at least

$$\tau^{\star} = \int_0^1 \frac{1}{a_0 + a_1 s + a_2 s^2}\,ds. \quad (113)$$

Thus, $t_{k+1}^{\star} - t_k' \geq \tau^{\star}$. Since $t_{k+1} > t_{k+1}^{\star}$ and $t_{k+1} - t_k \geq t_{k+1} - t_k'$, we obtain that $t_{k+1} - t_k \geq \tau^{\star}$. Hence $\tau^{\star}$ is a lower bound of the inter-execution times. It can be considered as a *minimal dwell-time*, which is independent on the initial condition of the system. This concludes the proof. ∎

Remark 5. Since there is a minimal dwell-time (which is uniform and does not depend on initial conditions), no Zeno solution can appear. This has a very important consequence as it allows to guarantee the existence and uniqueness of the closed-loop solution. The solution, can be constructed by the step method. We omit the details of well-posedness in this article, but we refer to References 37 and 57 for further details on the notion of solutions under an hybrid control scheme.

5.2 | Lyapunov-based analysis

To prove the exponential convergence of the closed-loop system with the event-triggered control law (96)–(98), perform a Lyapunov-based analysis on the target systems (52)–(56) and (59)–(63).

Theorem 2. *Let $\kappa_{\hat{\alpha}_1}$, $\kappa_{\hat{\beta}_2}$, $\kappa_{\hat{\beta}_1}$, $\kappa_{\hat{\alpha}_2}$, $\kappa_{\tilde{\alpha}_1}$ be the parameters introduced in (72)–(76) (related to traffic modeling and boundary control gains). Let ϱ_i^+, ϱ_i^-, C be given in (86)–(88) and (93), respectively, and assume μ sufficiently small such that conditions (82)–(85) hold.*
  Let $\theta_0, \theta_2 > 0$, $\sigma \in (0,1)$ and θ_1 (in 95) be selected in such a way that

  (i) condition (106) is met, and

(ii) the following conditions are fulfilled:

$$2\varrho_1^- \exp\left(\frac{\mu L}{\gamma_1 p_1^\star - v_1^\star}\right)\left(r_1 \exp\left(\frac{-L}{\tau_1 v_1^\star}\right)\right)^2 - \varrho_1^+ \exp\left(\frac{-\mu L}{v_1^\star}\right) + \max\left\{\frac{2}{C}\theta_1\theta_2\kappa_{\hat{\alpha}_1}, \frac{\theta_0}{2} + 2\theta_1\theta_2\kappa_{\tilde{\alpha}_1}\right\} < 0, \quad (114)$$

$$\varrho_2^- \exp\left(\frac{\mu L}{v_2^\star}\right)\left(\frac{1}{r_2}\exp\left(\frac{-L}{\tau_2 v_2^\star}\right)\right)^2 - \varrho_2^+ \exp\left(\frac{-\mu L}{\gamma_2 p_2^\star - v_2^\star}\right) + \frac{2}{C}\theta_1\theta_2\kappa_{\hat{\beta}_2} < 0, \quad (115)$$

$$2\left((\delta\frac{r_2}{r_1})^2 + \frac{1}{C}\theta_1\theta_2\kappa_{\hat{\beta}_1}\right)\varrho_2^+ - \varrho_1^- < 0, \quad (116)$$

$$2\left((1-\delta)^2 r_2^2 + \frac{1}{C}\theta_1\theta_2\kappa_{\hat{\alpha}_2}\right)\varrho_2^+ + \varrho_1^+ - \varrho_2^- < 0. \quad (117)$$

Then, the closed-loop system (28)–(31), (44) with the observer-based event-triggered boundary control (96)–(98) is exponentially convergent in the L^2-norm.

Remark 6. The sufficient conditions for exponential convergence (114)–(117) essentially rely on the conditions (82)–(85). The suitable selection of the parameters to meet these conditions greatly affects the event-triggered strategy in terms of sampling frequency and convergence performance. For example, notice that if the parameters $\kappa_{\hat{\alpha}_1}$, $\kappa_{\hat{\beta}_2}$, $\kappa_{\hat{\beta}_1}$, $\kappa_{\hat{\alpha}_2}$, $\kappa_{\tilde{\alpha}_1}$ (see Table 1) related to the control gains are large (meaning that suppressing the stop-and-go oscillation phenomenon requires high control effort), then we need either θ_1 or θ_2 to be sufficiently small. Hence, one may expect the dynamic variable to have more relevance (see Remarks 3 and 4) and thus make the event-triggered sampling to be less frequent. Besides, we have stated that μ -related to the decay rate- also has to be small, implying a degradation of the performance convergence. This is one of the main trade-offs that one may expect under an event-triggered control scheme.

Proof. Consider the following Lyapunov function candidate for the target systems (52)–(56) and (59)–(63) along with (97), defined for all $(\tilde{\alpha}_i(t, \cdot), \tilde{\beta}_i(t, \cdot)) \in L^2((0, L); \mathbb{R}^4)$, $(\hat{\alpha}_i(t, \cdot), \hat{\beta}_i(t, \cdot)) \in L^2((0, L); \mathbb{R}^4)$, and $m \in \mathbb{R}^-$ by

$$W = V - m, \quad (118)$$

where V is given by (92) and m is the solution to (97). Taking the time derivative of (118) along the respective solutions, we get

$$\dot{W}(t) = -\mu V(t) + \mu(1 - \sigma)m(t) - \theta_1 d^2(t) + \frac{\mu}{2}\sigma V(t) + 2\theta_1\theta_2$$

$$\left(\kappa_{\hat{\alpha}_1}\hat{\alpha}_1^2(t, L) + \kappa_{\hat{\beta}_2}\hat{\beta}_2^2(t, L) + \kappa_{\hat{\beta}_1}\hat{\beta}_1^2(t, 0) + \kappa_{\hat{\alpha}_2}\hat{\alpha}_2^2(t, 0) + \kappa_{\tilde{\alpha}_1}\tilde{\alpha}_1^2(t, L)\right)$$

$$-\begin{pmatrix}\tilde{\alpha}_1(t, L) \\ \tilde{\beta}_2(t, L)\end{pmatrix}^\top Q^+(\mu L)\begin{pmatrix}\tilde{\alpha}_1(t, L) \\ \tilde{\beta}_2(t, L)\end{pmatrix} + \begin{pmatrix}\tilde{\alpha}_1(t, 0) \\ \tilde{\beta}_2(t, 0)\end{pmatrix}^\top Q^+(0)\begin{pmatrix}\tilde{\alpha}_1(t, 0) \\ \tilde{\beta}_2(t, 0)\end{pmatrix} + \begin{pmatrix}\tilde{\beta}_1(t, L) \\ \tilde{\alpha}_2(t, L)\end{pmatrix}^\top Q^-(\mu L)\begin{pmatrix}\tilde{\beta}_1(t, L) \\ \tilde{\alpha}_2(t, L)\end{pmatrix}$$

$$-\begin{pmatrix}\tilde{\beta}_1(t, 0) \\ \tilde{\alpha}_2(t, 0)\end{pmatrix}^\top Q^-(0)\begin{pmatrix}\tilde{\beta}_1(t, 0) \\ \tilde{\alpha}_2(t, 0)\end{pmatrix} - C\begin{pmatrix}\hat{\alpha}_1(t, L) \\ \hat{\beta}_2(t, L)\end{pmatrix}^\top Q^+(\mu L)\begin{pmatrix}\hat{\alpha}_1(t, L) \\ \hat{\beta}_2(t, L)\end{pmatrix} + C\begin{pmatrix}\hat{\alpha}_1(t, 0) \\ \hat{\beta}_2(t, 0)\end{pmatrix}^\top Q^+(0)\begin{pmatrix}\hat{\alpha}_1(t, 0) \\ \hat{\beta}_2(t, 0)\end{pmatrix}$$

$$+C\begin{pmatrix}\hat{\beta}_1(t, L) \\ \hat{\alpha}_2(t, L)\end{pmatrix}^\top Q^-(\mu L)\begin{pmatrix}\hat{\beta}_1(t, L) \\ \hat{\alpha}_2(t, L)\end{pmatrix} - C\begin{pmatrix}\hat{\beta}_1(t, 0) \\ \hat{\alpha}_2(t, 0)\end{pmatrix}^\top Q^-(0)\begin{pmatrix}\hat{\beta}_1(t, 0) \\ \hat{\alpha}_2(t, 0)\end{pmatrix}$$

$$+2C\tilde{\alpha}_1(t, L)\left(\int_0^L \begin{pmatrix}\hat{\alpha}_1(x) \\ \hat{\beta}_2(x)\end{pmatrix}^\top (\Lambda^+)^{-1}Q^+(\mu x)\begin{pmatrix}p_{\mu_1}(x) \\ p_{v_2}(x)\end{pmatrix}dx + \int_0^L \begin{pmatrix}\hat{\beta}_1(x) \\ \hat{\alpha}_2(x)\end{pmatrix}^\top (\Lambda^-)^{-1}Q^-(\mu x)\begin{pmatrix}p_{v_1}(x) \\ p_{\mu_2}(x)\end{pmatrix}dx\right), \quad (119)$$

where, $Q^+(\mu x), Q^-(\mu x)$ are given in (81) along with the explicit characterization given in (86)–(88) and μ sufficiently small.

Using the Young's inequality and the boundary conditions (56) and (63) with G given by (33) and which is here rewritten as

$$G = \begin{pmatrix} 0_{2\times2} & G_{01} \\ G_{10} & 0_{2\times2} \end{pmatrix},$$

with

$$G_{01} = \begin{pmatrix} 0 & 1 \\ \delta \frac{r_2}{r_1} & (1-\delta)r_2 \end{pmatrix}, \quad G_{10} = \begin{pmatrix} r_1 \exp\left(\frac{-L}{\tau_1 v_1^\star}\right) & 0 \\ 0 & \frac{1}{r_2} \exp\left(\frac{-L}{\tau_2 v_2^\star}\right) \end{pmatrix},$$

we obtain from (119) the following estimate:

$$\dot{W}(t) \leq -\mu\left(1 - \frac{\sigma}{2}\right)V(t) + \frac{C}{\chi_2}V_2(t) + \mu(1-\sigma)m(t) - \theta_1 d^2(t) + \left(\left(\frac{1-r_1^\star}{\rho}\right)_1 + \frac{r_1}{\chi_1}\exp\left(\frac{-L}{\tau_1 v_1^\star}\right)\right)$$

$$C\varrho_1^- \exp\left(\frac{\mu L}{\gamma_1 p_1^\star - v_1^\star}\right)\left(\frac{1-r_1}{\rho_1^\star}\right)d^2(t)$$

$$+ \begin{pmatrix} \tilde{\alpha}_1(t,L) \\ \tilde{\beta}_2(t,L) \end{pmatrix}^\top [G_{10}^\top Q^-(\mu L)G_{10} - Q^+(\mu L)]\begin{pmatrix} \tilde{\alpha}_1(t,L) \\ \tilde{\beta}_2(t,L) \end{pmatrix} + \begin{pmatrix} \tilde{\beta}_1(t,0) \\ \tilde{\alpha}_2(t,0) \end{pmatrix}^\top [G_{01}^\top Q^+(0)G_{01} - Q^-(0)]\begin{pmatrix} \tilde{\beta}_1(t,0) \\ \tilde{\alpha}_2(t,0) \end{pmatrix}$$

$$+ \begin{pmatrix} \hat{\alpha}_1(t,L) \\ \hat{\beta}_2(t,L) \end{pmatrix}^\top C[G_{10}^\top Q^-(\mu L)G_{10} - Q^+(\mu L)]\begin{pmatrix} \hat{\alpha}_1(t,L) \\ \hat{\beta}_2(t,L) \end{pmatrix} + \begin{pmatrix} \hat{\beta}_1(t,0) \\ \hat{\alpha}_2(t,0) \end{pmatrix}^\top C[G_{01}^\top Q^+(0)G_{01} - Q^-(0)]\begin{pmatrix} \hat{\beta}_1(t,0) \\ \hat{\alpha}_2(t,0) \end{pmatrix}$$

$$+ \chi_1 C r_1 \exp\left(\frac{-L}{\tau_1 v_1^\star}\right)\varrho_1^- \exp\left(\frac{\mu L}{\gamma_1 p_1^\star - v_1^\star}\right)\left(\frac{1-r_1}{\rho_1^\star}\right)\hat{\alpha}_1^2(t,L) + \chi_2 C C_0 \tilde{\alpha}_1^2(t,L)$$

$$+ 2\theta_1\theta_2\left(\kappa_{\hat{\alpha}_1}\hat{\alpha}_1^2(t,L) + \kappa_{\hat{\beta}_2}\hat{\beta}_2^2(t,L) + \kappa_{\hat{\beta}_1}\hat{\beta}_1^2(t,0) + \kappa_{\hat{\alpha}_2}\hat{\alpha}_2^2(t,0) + \kappa_{\tilde{\alpha}_1}\tilde{\alpha}_1^2(t,L)\right), \tag{120}$$

where C and C_0 are defined in (93)–(94) and χ_1 and χ_2 are any positive parameter that, in particular, can be set as $\chi_1 = r_1 \exp\left(\frac{-L}{\tau_1 v_1^\star}\right)\left(\frac{\rho_1^\star}{1-r_1}\right)$ and $\chi_2 = \frac{2}{\mu}$. Moreover, since θ_1 is given by (95), we then obtain the following estimate:

$$\dot{W}(t) \leq -\frac{\mu}{2}(1-\sigma)V(t) - \frac{\mu}{2}V_1(t) + \mu(1-\sigma)m(t)$$

$$+ \begin{pmatrix} \tilde{\alpha}_1(t,L) \\ \tilde{\beta}_2(t,L) \end{pmatrix}^\top [G_{10}^\top Q^-(\mu L)G_{10} - Q^+(\mu L)]\begin{pmatrix} \tilde{\alpha}_1(t,L) \\ \tilde{\beta}_2(t,L) \end{pmatrix} + \begin{pmatrix} \tilde{\beta}_1(t,0) \\ \tilde{\alpha}_2(t,0) \end{pmatrix}^\top [G_{01}^\top Q^+(0)G_{01} - Q^-(0)]\begin{pmatrix} \tilde{\beta}_1(t,0) \\ \tilde{\alpha}_2(t,0) \end{pmatrix}$$

$$+ \begin{pmatrix} \hat{\alpha}_1(t,L) \\ \hat{\beta}_2(t,L) \end{pmatrix}^\top C[G_{10}^\top Q^-(\mu L)G_{10} - Q^+(\mu L)]\begin{pmatrix} \hat{\alpha}_1(t,L) \\ \hat{\beta}_2(t,L) \end{pmatrix} + \begin{pmatrix} \hat{\beta}_1(t,0) \\ \hat{\alpha}_2(t,0) \end{pmatrix}^\top C[G_{01}^\top Q^+(0)G_{01} - Q^-(0)]\begin{pmatrix} \hat{\beta}_1(t,0) \\ \hat{\alpha}_2(t,0) \end{pmatrix}$$

$$+ \left(C r_1^2 \exp\left(\frac{-2L}{\tau_1 v_1^\star}\right)\varrho_1^- \exp\left(\frac{\mu L}{\gamma_1 p_1^\star - v_1^\star}\right) + 2\theta_1\theta_2\kappa_{\hat{\alpha}_1}\right)\hat{\alpha}_1^2(t,L) + \left(\frac{\theta_0}{2} + 2\theta_1\theta_2\kappa_{\tilde{\alpha}_1}\right)\tilde{\alpha}_1^2(t,L)$$

$$+ 2\theta_1\theta_2\left(\kappa_{\hat{\beta}_2}\hat{\beta}_2^2(t,L) + \kappa_{\hat{\beta}_1}\hat{\beta}_1^2(t,0) + \kappa_{\hat{\alpha}_2}\hat{\alpha}_2^2(t,0)\right). \tag{121}$$

Recall that under Assumption 1, if the more conservative conditions (82)–(85) are satisfied (with μ sufficiently small and $\varrho_i^+, \varrho_i^-, i = 1, 2$ explicitly characterized in 86–89), it holds that the LMIs appearing in (121), are verified as well, that is,

$$G_{01}^\top Q^+(0)G_{01} - Q^-(0) < 0,$$

$$G_{10}^\top Q^-(\mu L)G_{10} - Q^+(\mu L) < 0.$$

However, in order to compensate the last terms in (121), we need to rewrite (121) in a more compact form and analyze the resulting boundary terms. Therefore,

$$\dot{W}(t) \leq -\frac{\mu}{2}(1-\sigma)W(t) + \frac{\mu}{2}(1-\sigma)m(t)$$

$$+ \begin{pmatrix} \tilde{\alpha}_1(t,L) \\ \tilde{\beta}_2(t,L) \end{pmatrix}^\top [G_{10}^\top Q^-(\mu L)G_{10} - Q^+(\mu L) + \mathcal{D}_0]\begin{pmatrix} \tilde{\alpha}_1(t,L) \\ \tilde{\beta}_2(t,L) \end{pmatrix} + \begin{pmatrix} \tilde{\beta}_1(t,0) \\ \tilde{\alpha}_2(t,0) \end{pmatrix}^\top [G_{01}^\top Q^+(0)G_{01} - Q^-(0)]\begin{pmatrix} \tilde{\beta}_1(t,0) \\ \tilde{\alpha}_2(t,0) \end{pmatrix}$$

$$
+ \begin{pmatrix} \hat{\alpha}_1(t,L) \\ \hat{\beta}_2(t,L) \end{pmatrix}^\top C[G_{10}^\top Q^-(\mu L)G_{10}
$$

$$
- Q^+(\mu L) + \mathcal{D}_1] \begin{pmatrix} \hat{\alpha}_1(t,L) \\ \hat{\beta}_2(t,L) \end{pmatrix} + \begin{pmatrix} \hat{\beta}_1(t,0) \\ \hat{\alpha}_2(t,0) \end{pmatrix}^\top C[G_{01}^\top Q^+(0)G_{01} - Q^-(0) + \mathcal{D}_2] \begin{pmatrix} \hat{\beta}_1(t,0) \\ \hat{\alpha}_2(t,0) \end{pmatrix}, \tag{122}
$$

where

$$
\mathcal{D}_0 = \begin{pmatrix} \frac{\theta_0}{2} + 2\theta_1\theta_2\kappa_{\tilde{\alpha}_1} & 0 \\ 0 & 0 \end{pmatrix}, \tag{123}
$$

$$
\mathcal{D}_1 = \frac{1}{C} \begin{pmatrix} \varrho_1^- C r_1^2 \exp\left(\frac{-2L}{\tau_1 v_1^\star} + \frac{\mu L}{\gamma_1 p_1^\star - v_1^\star} \right) + 2\theta_1\theta_2\kappa_{\hat{\alpha}_1} & 0 \\ 0 & 2\theta_1\theta_2\kappa_{\hat{\beta}_2} \end{pmatrix}, \tag{124}
$$

$$
\mathcal{D}_2 = \frac{1}{C} \begin{pmatrix} 2\theta_1\theta_2\kappa_{\hat{\beta}_1} & 0 \\ 0 & 2\theta_1\theta_2\kappa_{\hat{\alpha}_2} \end{pmatrix}. \tag{125}
$$

We require the following LMI-like conditions to hold:

$$
G_{10}^\top Q^-(\mu L)G_{10} - Q^+(\mu L) + \mathcal{D}_0 < 0, \tag{126}
$$

$$
G_{10}^\top Q^-(\mu L)G_{10} - Q^+(\mu L) + \mathcal{D}_1 < 0, \tag{127}
$$

$$
G_{01}^\top Q^+(0)G_{01} - Q^-(0) + \mathcal{D}_2 < 0. \tag{128}
$$

Notice that if (128) holds, then $G_{01}^\top Q^+(0)G_{01} - Q^-(0) < 0$ immediately holds as well. Now, it should be noticed that conditions (126)–(128) are verified provided that the (more conservative) conditions (114)–(117) hold. This is true since we can invoke conditions (82)–(85) (which hold by virtue of Assumption 1 as discussed in Section 4.1) and we can select θ_0 (in turn θ_1), μ sufficiently small and choose θ_2 such that (106) is verified. Therefore, from (122) and in light of conditions (114)–(117), we get

$$
\dot{W}(t) \leq -\frac{\mu}{2}(1-\sigma)W(t) + \frac{\mu}{2}(1-\sigma)m(t). \tag{129}
$$

By Lemma 1 in conjunction with Theorem 1, we guarantee that $m(t) < 0$ for all $t > 0$ (since we can assert now that $\lim_{k\to\infty}(t_k) = +\infty$). Thus we finally obtain

$$
\dot{W}(t) \leq -\frac{\mu}{2}(1-\sigma)W(t).
$$

By the comparison principle, and remarking that $V \leq W$, we have, for all $t \geq 0$,

$$
V(t) \leq \exp\left(-\frac{\mu}{2}(1-\sigma)t \right)(V(0) - m^0). \tag{130}
$$

By recalling also that there exist $\underline{\varpi}$, $\overline{\varpi}$ (depending on ϱ_i^+, ϱ_i^- and on μ) such that $\underline{\varpi}\|(\tilde{\alpha}_i(t,\cdot), \tilde{\beta}_i(t,\cdot), \hat{\alpha}_i(t,\cdot), \hat{\beta}_i(t,\cdot))\|_{L^2}^2 \leq V \leq \overline{\varpi}\|(\tilde{\alpha}_i(t,\cdot), \tilde{\beta}_i(t,\cdot), \hat{\alpha}_i(t,\cdot), \hat{\beta}_i(t,\cdot))\|_{L^2}^2$, $i = 1, 2$, we obtain for all $t \geq 0$,

$$
\|(\tilde{\alpha}_i(t,\cdot), \tilde{\beta}_i(t,\cdot))\|_{L^2}^2 + \|(\hat{\alpha}_i(t,\cdot), \hat{\beta}_i(t,\cdot))\|_{L^2}^2 \leq \frac{\overline{\varpi}}{\underline{\varpi}}\exp\left(-\frac{\mu}{2}(1-\sigma)t \right)\left(\|(\tilde{\alpha}_i^0, \tilde{\beta}_i^0)\|_{L^2}^2 + \|(\hat{\alpha}_i^0, \hat{\beta}_i^0)\|_{L^2}^2 \right)\frac{1}{\underline{\varpi}}\exp\left(-\frac{\mu}{2}(1-\sigma)t \right)m^0.
$$

Using (51), (68), (58), and (57) and their bounded invertibility, it can be shown that there exist $\overline{\mathcal{N}}$, $\overline{\mathcal{L}}$, $\overline{\mathcal{R}}$, and $\overline{\mathcal{K}}$ such that the following norm equivalences hold:

$$\|(\tilde{w}_i(t,\cdot),\tilde{v}_i(t,\cdot))\|_{L^2}^2 \leq \overline{\mathcal{N}}\|(\tilde{\alpha}_i(t,\cdot),\tilde{\beta}_i(t,\cdot))\|_{L^2}^2,$$

$$\|(\hat{w}_i(t,\cdot),\hat{v}_i(t,\cdot))\|_{L^2}^2 \leq \overline{\mathcal{L}}\|(\hat{\alpha}_i(t,\cdot),\hat{\beta}_i(t,\cdot))\|_{L^2}^2,$$

$$\|(\tilde{\alpha}_i(t,\cdot),\tilde{\beta}_i(t,\cdot))\|_{L^2}^2 \leq \overline{\mathcal{R}}\|(\tilde{w}_i(t,\cdot),\tilde{v}_i(t,\cdot))\|_{L^2}^2,$$

$$\|(\hat{\alpha}_i(t,\cdot),\hat{\beta}_i(t,\cdot))\|_{L^2}^2 \leq \overline{\mathcal{K}}\|(\hat{w}_i(t,\cdot),\hat{v}_i(t,\cdot))\|_{L^2}^2.$$

Therefore, it holds

$$\min\left\{\frac{1}{\overline{\mathcal{L}}},\frac{1}{\overline{\mathcal{N}}}\right\}\left(\|(\hat{w}_i(t,\cdot),\hat{v}_i(t,\cdot))\|_{L^2}^2 + \|(\tilde{w}_i(t,\cdot),\tilde{v}_i(t,\cdot))\|_{L^2}^2\right) \leq \frac{\overline{\varpi}}{\underline{\varpi}}\exp\left(-\frac{\mu}{2}(1-\sigma)t\right)\left(\overline{\mathcal{K}}\|(\hat{w}_i^0,\hat{v}_i^0)\|_{L^2}^2 + \overline{\mathcal{R}}\|(\tilde{w}_i^0,\tilde{v}_i^0)\|_{L^2}^2\right)$$
$$-\frac{1}{\underline{\varpi}}\exp\left(-\frac{\mu}{2}(1-\sigma)t\right)m^0. \tag{131}$$

Further, it holds that $\|(\overline{w}_i(t,\cdot),\overline{v}_i(t,\cdot))\|_{L^2}^2 \leq 2\|(\hat{w}_i(t,\cdot),\hat{v}_i(t,\cdot))\|_{L^2}^2 + 2\|(\tilde{w}_i(t,\cdot),\tilde{v}_i(t,\cdot))\|_{L^2}^2$ and $\|(\tilde{w}_i(t,\cdot),\tilde{v}_i(t,\cdot))\|_{L^2}^2 \leq 2\|(\hat{w}_i(t,\cdot),\hat{v}_i(t,\cdot))\|_{L^2}^2 + 2\|(\overline{w}_i(t,\cdot),\overline{v}_i(t,\cdot))\|_{L^2}^2$; thus we have, on the one hand

$$\frac{1}{2}\min\left\{\frac{1}{\overline{\mathcal{L}}},\frac{1}{\overline{\mathcal{N}}}\right\}\|(\overline{w}_i(t,\cdot),\overline{v}_i(t,\cdot))\|_{L^2}^2$$
$$\leq \frac{\overline{\varpi}}{\underline{\varpi}}\exp\left(-\frac{\mu}{2}(1-\sigma)t\right)\left(\overline{\mathcal{K}}\|(\hat{w}_i^0,\hat{v}_i^0)\|_{L^2}^2 + 2\overline{\mathcal{R}}\|(\hat{w}_i^0,\hat{v}_i^0)\|_{L^2}^2 + 2\overline{\mathcal{R}}\|(\overline{w}_i^0,\overline{v}_i^0)\|_{L^2}^2\right) - \frac{1}{\underline{\varpi}}\exp\left(-\frac{\mu}{2}(1-\sigma)t\right)m^0,$$

and on the other hand,

$$\frac{1}{2}\min\left\{\frac{1}{\overline{\mathcal{L}}},\frac{1}{\overline{\mathcal{N}}}\right\}\|(\hat{w}_i(t,\cdot),\hat{v}_i(t,\cdot))\|_{L^2}^2$$
$$\leq \frac{\overline{\varpi}}{\underline{\varpi}}\exp\left(-\frac{\mu}{2}(1-\sigma)t\right)\left(\overline{\mathcal{K}}\|(\hat{w}_i^0,\hat{v}_i^0)\|_{L^2}^2 + 2\overline{\mathcal{R}}\|(\hat{w}_i^0,\hat{v}_i^0)\|_{L^2}^2 + 2\overline{\mathcal{R}}\|(\overline{w}_i^0,\overline{v}_i^0)\|_{L^2}^2\right) - \frac{1}{\underline{\varpi}}\exp\left(-\frac{\mu}{2}(1-\sigma)t\right)m^0.$$

Finally, we obtain the following estimate

$$\|(\overline{w}_i(t,\cdot),\overline{v}_i(t,\cdot))\|_{L^2}^2 + \|(\hat{w}_i(t,\cdot),\hat{v}_i(t,\cdot))\|_{L^2}^2 \leq \mathcal{M}_1\exp\left(-\frac{\mu}{2}(1-\sigma)t\right)$$
$$\left(\|(\overline{w}_i^0,\overline{v}_i^0)\|_{L^2}^2 + \|(\hat{w}_i^0,\hat{v}_i^0)\|_{L^2}^2\right) - \mathcal{M}_2\exp\left(-\frac{\mu}{2}(1-\sigma)t\right)m^0,$$

with $\mathcal{M}_1 = 2\frac{\overline{\varpi}}{\underline{\varpi}}\frac{\max\left\{2\overline{\mathcal{R}},2\overline{\mathcal{R}}+\overline{\mathcal{K}}\right\}}{\min\left\{\frac{1}{\overline{\mathcal{L}}},\frac{1}{\overline{\mathcal{N}}}\right\}}$ and $\mathcal{M}_2 = 2\frac{1}{\underline{\varpi}}\frac{\max\left\{2\overline{\mathcal{R}},2\overline{\mathcal{R}}+\overline{\mathcal{K}}\right\}}{\min\left\{\frac{1}{\overline{\mathcal{L}}},\frac{1}{\overline{\mathcal{N}}}\right\}}$. This concludes the proof. ∎

Remark 7. In Theorem 2, we have established the exponential convergence of the closed-loop system to the equilibrium point. We could have obtained exponential stability if we set $m^0 = 0$. However, if $m^0 = 0$, then $m(t) \leq 0$. Then, the function $\psi^\star(t)$ in (108) is not defined when $m(t) = 0$. Therefore, the existence of a minimal-dwell time may not be proved easily by following the same arguments as in the proof of Theorem 1. Hence, in this article we opted to choose m^0 strictly negative.

6 | NUMERICAL SIMULATIONS

In this section, we validate the event-triggered strategy with numerical simulations. The length of each freeway segment is chosen to be $L = 1$ km so the total length of the two connected segments are 2 km. The maximum speed limit is $v_m = 40$ $m/s = 144$ km/h. We consider 6 lanes for the downstream freeway segment 1. Assuming the average vehicle length is 5 m plus the minimum safety distance of 50% vehicle length, the maximum density of the road is obtained as $\rho_{m,1} = 800$ *vehicles/km*. The upstream segment has less functional lanes thus its maximum density is $\rho_{m,2} = 700$ *vehicles/km*. We take $\gamma_i = 0.5$. The ratio of the characteristic speeds are $r_1 = -0.44$, $r_2 = -0.64$. The steady
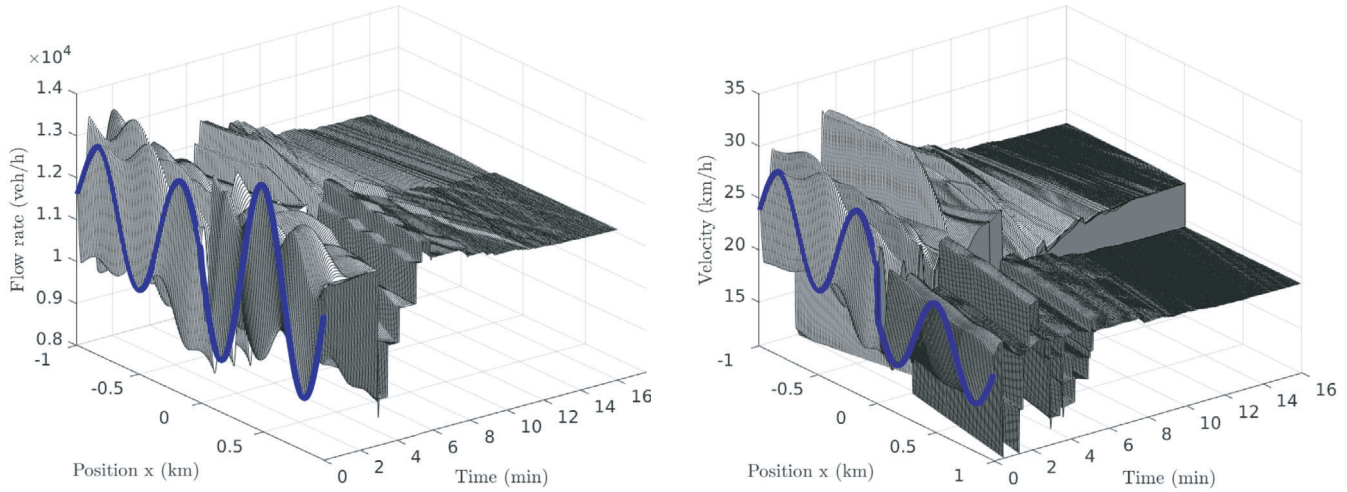
FIGURE 5 Numerical solution of the flow rate and velocity with the ramp metering event-triggered boundary control $U_{\text{nom}}(t_k)$ (96)–(98)
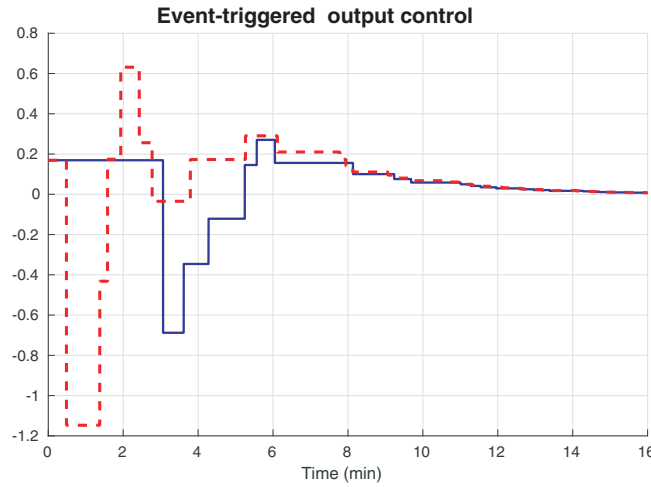

FIGURE 6 Time-evolution of the event-triggered boundary output control. The updating is aperiodically, according to the dynamic triggering condition (96), under the cases (i) $\theta_2 = 1.98$ (blue line) and (ii) $\theta_2 = 10^9$ (red dashed-line) which corresponds to the limiting case in which one deals with a " static triggering condition" as discussed in Remark 3

states $(\rho_1^\star, v_1^\star)$ and $(\rho_2^\star, v_2^\star)$ are chosen respectively as $(600 \; vehicles/km, 19.4 \; km/h)$ and $(488.6 \; vehicles/km, 23.8 \; km/h)$, both of which are in the congested regime. The constant flow rate is $q^\star = \rho_1^\star v_1^\star = \rho_2^\star v_2^\star = 11,640 \; vehicles/h$, same for the two segments. If we consider the segment 1 with 6 lanes, then the averaged flow rate of each lane is $1940 \; vehicles/h/lane$. The equilibrium steady state of the downstream road has higher density and lower velocity, thus is more congested than the upstream road. The relaxation time is $\tau_1 = 90 \; s$ and $\tau_2 = 60 \; s$.

We use sinusoid initial conditions for flow rate and velocity field which represent the initial stop-and-go oscillations on the connected freeway. We perform the simulation on a time horizon of 16 min. We apply a two-step Lax-Wendroff numerical scheme[62] is applied.

Event-triggered implementation and closed-loop simulation

The parameters related to the control gains (see Table 1) are, $\kappa_{\hat{\alpha}_1} = 1.37$, $\kappa_{\hat{\beta}_1} = 23.8$, $\kappa_{\hat{\alpha}_2} = 18.68$, $\kappa_{\hat{\beta}_2} = 1.79$, $\kappa_{\tilde{\alpha}_1} = 19.7 \times 10^2$, $\varepsilon_0 = 6.4 \times 10^{-3}$, $\varepsilon_1 = 4.08 \times 10^{-3}$. Those related to the observer-based event-triggering boundary controller are selected as $\theta_0 = 0.01$, $\theta_1 = 1.42 \times 10^{-9}$, $\theta_2 = 1.98$, $\sigma = 0.05$, $\mu = 5 \times 10^{-3}$. Moreover, using the previous parameters in conjunction with $\varrho_1^+ = 6.58$, $\varrho_2^+ = 2.71$, $\varrho_1^- = 98.64$, $\varrho_2^- = 10.5$ obtained using (86)–(89), and $C = 41 \times 10^{-4}$ in (93), one

can verify that conditions (106) and (114)–(117) hold. Hence, Theorem 2 applies. Moreover, we compute the minimal dwell-time between two triggering times according to (113), that is $\tau^\star = 32.4$ s. We stabilize the system on events under the event-triggered boundary control (98), (96). Figure 5 shows the numerical solution of flow rate and velocity with the ramp metering event-triggered output control $U_{\text{nom}}(t_k)$ which is updated according to the observer-based event-triggered boundary control (96). Figure 6 shows, in blue line, the time-evolution of the control signal (recall that designed controller U_{nom} is the flow rate perturbation around a nominal flow rate), where we can observe that the updating is aperiodically, only when needed. We highlight also the case when θ_2 is very large so the triggering condition corresponds to the limiting case of a "static" one (see discussion in Remark 3). As expected, under a static triggering condition one samples faster and obtain shorter inter-execution times than under a dynamic triggering condition.

7 | CONCLUSION

In this article, we have designed an event-triggered boundary control that guarantees the simultaneous stabilization of the traffic flow on two cascaded roads around given steady states. The nominal output-feedback law is adjusted from Reference 20 and has been designed using the backstepping methodology on the linearized ARZ model. The flow actuation is realized with the ramp metering at the downstream outlet. The measurements are collocated. The updating of the control signal is done according to a suitable dynamic triggering condition. We proved that under this strategy, there exists a uniform minimal dwell-time (independent of initial conditions), thus avoiding the Zeno phenomenon. We also guaranteed the exponential convergence of the closed-loop system under the proposed event-triggered boundary control. The resulting suitably sampled control law is avoids useless actuation solicitations. Future work includes the design of periodic event-triggered control strategy to monitor the triggering condition periodically, hence, saving computational resources. Moreover, the questions related to quantized implementations of event-triggered controllers will also be considered. They will lay the foundations for digital realizations of boundary backstepping-based controllers. In that prospect, the approach proposed in Reference 63 may be a relevant path to follow.

CONFLICT OF INTEREST
There is no conflict of interests for this article.

DATA AVAILABILITY STATEMENT
Data sharing not applicable to this article as no datasets were generated or analyzed during the current study

ENDNOTES
*See also References 56,57, and 9 (section 3) for further details of sufficient conditions for exponential stability and Lyapunov-based techniques for 1D linear hyperbolic systems.

†For more general linear hyperbolic systems, for example, higher number of states, complex boundary interconnections, or balance laws terms, one can formulate an optimization problem with LMIs to find $Q^+(\mu x)$, $Q^-(\mu x)$ using semi-definite programming (SDP) combined with for example, a line search algorithm; hence verifying the feasibility of the resulting sufficient conditions for stability; see for instance Reference 57.

ORCID
Nicolas Espitia 🔟 https://orcid.org/0000-0001-8241-0633

REFERENCES
1. Lighthill M, Whitham G. On kinematic waves II. A theory of traffic flow on long crowded roads. *Proc Royal Soc Lond Ser A Math Phys Sci.* 1955;229(1178):317-345.
2. Richards P. Shock waves on the highway. *Operat Res.* 1956;4(1):42-51.
3. Aw A, Rascle M. Resurrection of "second order" models of traffic flow. *SIAM J Appl Math.* 2000;60(3):916-938.
4. Zhang HM. A non-equilibrium traffic model devoid of gas-like behavior. *Transp Res B Methodol.* 2002;36(3):275-290.
5. Flynn M, Kasimov A, Nave J, Rosales R, Seibold B. Self-sustained nonlinear waves in traffic flow. *Phys Rev E.* 2009;79(5):56-113.
6. Garavello M, Piccoli B. Traffic flow on a road network using the Aw–Rascle model. *Commun Part Differ Equ.* 2006;31(2):243-275.
7. Herty M, Rascle M. Coupling conditions for a class of second-order models for traffic flow. *SIAM J Math Anal.* 2006;38(2):595-616.
8. Siri S, Pasquale C, Sacone S, Ferrara A. Freeway traffic control: a survey. *Automatica.* 2021;130:109655.
9. Bastin G, Coron J-M. *Stability and Boundary Stabilization of 1-D Hyperbolic Systems.* Birkhäuser; 2016.
10. Karafyllis I, Papageorgiou M. Feedback control of scalar conservation laws with application to density control in freeways by means of variable speed limits. *Automatica.* 2019;105:228-236.

11. Yu H, Krstic M. Traffic congestion control for Aw-Rascle-Zhang model. *Automatica*. 2019;100:38-51.

12. Zhang L, Prieur C, Qiao J. PI boundary control of linear hyperbolic balance laws with stabilization of ARZ traffic flow models. *Syst Control Lett*. 2019;123:85-91.

13. Zhang L, Luan H, Lu Y, Prieur C. Boundary feedback stabilization of freeway traffic networks: ISS control and experiments. *IEEE Trans Control Syst Technol*. 2021;1-12.

14. Bekiaris-Liberis N, Delis AI. PDE-based feedback control of freeway traffic flow via time-gap manipulation of ACC-equipped vehicles. *IEEE Trans Control Syst Technol*. 2021;29(1):461-469.

15. Tumash L, Canudas de Wit C, Delle MM. Robust tracking control design for fluid traffic dynamics. 2019 IEEE 58th Conference on Decision and Control (CDC); 2019:4085-4090.

16. Di Meglio F, Vazquez R, Krstic M. Stabilization of a system of n+1 coupled first-order hyperbolic linear PDEs with a single boundary input. *IEEE Trans Automat Contr*. 2013;58(12):3097-3111.

17. Hu L, Di Meglio F, Vazquez R, Krstic M. Control of homodirectional and general heterodirectional linear coupled hyperbolic PDEs. *IEEE Trans Automat Contr*. 2016;61(11):3301-3314.

18. Auriol J, Di Meglio F. Minimum time control of heterodirectional linear coupled hyperbolic PDEs. *Automatica*. 2016;71:300-307.

19. Yu H, Gan Q, Bayen A, Krstic M. PDE traffic observer validated on freeway data. *IEEE Trans Control Syst Technol*. 2021;29(3).

20. Yu H, Auriol J, Krstic M. Simultaneous downstream and upstream output-feedback stabilization of cascaded freeway traffic. *Automatica*. 2022;136.

21. Auriol J, Di Meglio F, Bribiesca-Argomedo F. Delay robust state feedback stabilization of an underactuated networkof two interconnected PDE systems. Proceedings of the 2019 American Control Conference (ACC); 2019:593-599.

22. Fridman E, Blighovsky A. Robust sampled-data control of a class of semilinear parabolic systems. *Automatica*. 2012;48:826-836.

23. Karafyllis I, Krstic M. Sampled-data boundary feedback control of 1-D parabolic PDEs. *Automatica*. 2018;87:226-237.

24. Jiang A, Cui B, Wu W, Zhuang B. Event-driven observer-based control for distributed parameter systems using mobile sensor and actuator. *Comput Math Appl*. 2016;72:2854-2864.

25. Selivanov A, Fridman E. Distributed event-triggered control of transport-reaction systems. *Automatica*. 2016;68:344-351.

26. Yao Z, El-Farra NH. Resource-aware model predictive control of spatially distributed processes using event-triggered communication. Proceedings of the 52nd IEEE Conference on Decision and Control; 2013:3726-3731; IEEE.

27. Katz R, Fridman E, Selivanov A. Network-based boundary observer-controller design for 1D heat equation. Proceedings of the 58th IEEE Conference on Decision and Control (CDC); 2019; IEEE.

28. Katz R, Fridman E, Selivanov A. Boundary delayed observer-controller design for reaction-diffusion systems. *IEEE Trans Automat Contr*. 2021;66:275-282.

29. Espitia N, Karafyllis I, Krstic M. Event-triggered boundary control of constant-parameter reaction-diffusion PDEs: a small gain approach. *Automatica*. 2021;128:109562.

30. Karafyllis I, Espitia N, Krstic M. Event-triggered gain scheduling of reaction-diffusion PDEs. *SIAM J Control Optim*. 2021;59:2047-2067.

31. Logemann H, Rebarber R, Townley S. Generalized sampled-data stabilization of well-posed linear infinite-dimensional systems. *SIAM J Control Optim*. 2005;44:1345-1369.

32. Tan Y, Trélat E, Chitour Y, Neši D Dynamic practical stabilization of sampled-data linear distributed parameter systems. Proceedings of the IEEE 48th Conference on Decision and Control (CDC); 2009:5508-5513; IEEE.

33. Davo MA, Bresch-Pietri D, Prieur C, Di Meglio F. Stability analysis of a 2×2 linear hyperbolic system with a sampled-data controller via backstepping method and looped-functionals. *IEEE Trans Automat Contr*. 2018;64(4):1718-1725.

34. Karafyllis I, Krstic M. Sampled-data boundary feedback control of 1-D hyperbolic PDEs with non-local terms. *Syst Control Lett*. 2017;17:68-75.

35. Espitia N, Girard A, Marchand N, Prieur C. Event-based control of linear hyperbolic systems of conservation laws. *Automatica*. 2016;70:275-287.

36. Espitia N, Girard A, Marchand N, Prieur C. Event-based boundary control of a linear 2x2 hyperbolic system via backstepping approach. *IEEE Trans Automat Contr*. 2018;63(8):2686-2693.

37. Espitia N. Observer-based event-triggered boundary control of a linear 2 x 2 hyperbolic systems. *Syst Control Lett*. 2020;138.

38. Li X, Liu Y, Jian L, Fengzhong L. Adaptive event-triggered control for a class of uncertain hyperbolic PDE-ODE cascade systems. *Int J Robust Nonlinear Control*. 2021.

39. Wang J, Krstic M. Event-triggered output-feedback backstepping control of 2x2 hyperbolic PDE-ODE systems. *IEEE Trans Automat Contr*. 2021.

40. Tabuada P. Event-triggered real-time scheduling of stabilizing control tasks. *IEEE Trans Automat Contr*. 2007;52(9):1680-1685.

41. Heemels WPMH., Johansson KH., Tabuada P. An introduction to event-triggered and self-triggered control. Proceedings of the 51st IEEE Conference on Decision and Control; 2012:3270-3285; IEEE.

42. Marchand N, Durand S, Castellanos JFG. A general formula for event-based stabilization of nonlinear systems. *IEEE Trans Automat Contr*. 2013;58(5):1332-1337.

43. Lemmon M. *Event-Triggered Feedback in Control, Estimation, and Optimization*. Springer; 2010:293-358.

44. Girard A. Dynamic triggering mechanisms for event-triggered control. *IEEE Trans Automat Contr*. 2015;60(7):1992-1997.

45. Postoyan R, Tabuada P, Nesic D, Anta A. A framework for the event-triggered stabilization of nonlinear systems. *IEEE Trans Automat Contr*. 2015;60(4):982-996.

46. Liu T, Zhang P, Jiang Z-P. Event-triggered input-to-state stabilization of nonlinear systems subject to disturbances and dynamic uncertainties. *Automatica*. 2019;108:108488.

47. Ferrara A, Sacone S, Siri S. Event-triggered model predictive schemes for freeway traffic control. *Transp Res C*. 2015;59:554-567.

48. Ferrara A, Sacone S, Siri S. Design of networked freeway traffic controllers based on event-triggered control concepts. *Int J Robust Nonlinear Control*. 2016;26:1162-1183.

49. Pasquale C, Sacone S, Siri S, Ferrara A. Hierarchical centralized/decentralized event-triggered control of multiclass traffic networks. *IEEE Trans Control Syst Technol*. 2021;29(4):1549-1564.

50. Espitia N, Yu H, Krstic M. Event-triggered varying speed limit control for stop-and-go traffic. Proceedings of the IFAC World Congress; 2020.

51. Auriol J, Deutscher J, Mazanti G, Valmorbida G, eds. Ch. 11. Advances in distributed parameter systems, event-triggered output feedback control of traffic flow on cascaded roads. *Advances in Delays and Dynamics*. Springer; 2022.

52. Fan S, Seibold B. Data-fitted first-order traffic models and their second-order generalizations: comparison by trajectory and sensor data. *Transp Res Rec*. 2013;2391(1):32-43.

53. Yu H, Krstic M. Varying speed limit control of Aw-Rascle-Zhang Traffic model. Proceedings of the 21st International Conference on Intelligent Transportation Systems (ITSC); 2018:1846-1851.

54. Coron J-M, Hu L, Olive G. Stabilization and controllability of first-order integro-differential hyperbolic equations. *J Funct Anal*. 2016;271:554-3587.

55. Coron J-M, Bastin G, d'Andréa-Novel B. Dissipative boundary conditions for one-dimensional nonlinear hyperbolic systems. *SIAM J Control Optim*. 2008;47(3):1460-1498.

56. Diagne A, Bastin G, Coron J-M. Lyapunov exponential stability of 1-D linear hyperbolic systems of balance laws. *Automatica*. 2012;48(1):109-114.

57. Prieur C, Girard A, Witrant E. Stability of switched linear hyperbolic systems by Lyapunov techniques. *IEEE Trans Automat Contr*. 2014;59(8):2196-2202.

58. Auriol J, Di Meglio F. An explicit mapping from linear first order hyperbolic PDEs to difference systems. *Syst Control Lett*. 2019;123:144-150.

59. Hale J-K, Verduyn Lunel S-M. *Introduction to Functional Differential Equations*. Springer-Verlag; 1993.

60. Yoshida K. *Lectures on Differential and Integral Equations*. Interscience Publishers; 1960.

61. Rathnayake B, Diagne M, Espitia N, Karafyllis I. Observer-based event-triggered boundary control of a class of reaction-diffusion PDEs. *IEEE Trans Automat Contr*. 2021.

62. LeVeque RJ. *Finite Volume Methods for Hyperbolic Problems*. Cambridge University Press; 2002.

63. Bekiaris-Liberis N. Hybrid boundary stabilization of linear first-order hyperbolic PDEs despite almost quantized measurements and control input. *Syst Control Lett*. 2020;146:104809.

APPENDIX A. PDE-KERNEL EQUATIONS FOR CONTROL AND OBSERVER DESIGN

We recall that the sets $\mathcal{T}_1, \mathcal{T}_2$ are defined as :

$$\mathcal{T}_1 = \{(x, \xi) \in [0, L]^2, \xi \geq x\}, \; \mathcal{T}_2 = \{(x, \xi) \in [0, L]^2, \xi \leq x\},$$

and, the set $\mathcal{T}_3$ is defined as the unit square $[0, L]^2$: $\mathcal{T}_3 = \{(x, \xi) \in [0, L]^2\}$.

A.1 Kernels of backstepping transformation (51)

The kernels $N_1^{\alpha\alpha}$, $N_1^{\alpha\beta}$ are on $\mathcal{T}_1$, the kernels $N_2^{\alpha\alpha}$, $N_2^{\alpha\beta}$ are defined on $\mathcal{T}_2$, and the kernels N^α, N^β are defined on $\mathcal{T}_3$. The objective is to map the error system (46)–(50) to the target system (52)–(56) . Differentiating equation (51) with respect to time and space, and integrating by parts, we obtain the following set of kernel equations:

$$\partial_x N_i^{\alpha\alpha}(x, \xi) + \partial_\xi N_i^{\alpha\alpha}(x, \xi) = 0, \tag{A1}$$

$$(\gamma_1 p_1^\star - v_1^\star)\partial_x N_1^{\beta\alpha}(x, \xi) - v_1^\star \partial_\xi N_1^{\beta\alpha}(x, \xi) = -c_1(x)N_1^{\alpha\alpha}(x, \xi), \tag{A2}$$

$$(\gamma_2 p_2^\star - v_2^\star)\partial_x N_2^{\beta\alpha}(x, \xi) - v_2^\star \partial_\xi N_2^{\beta\alpha}(x, \xi) = c_2(x)N_2^{\alpha\alpha}(x, \xi), \tag{A3}$$

$$v_2^\star \partial_x N^\alpha(x,\xi) - v_1^\star \partial_\xi N^\alpha(x,\xi) = 0, \tag{A4}$$

$$(\gamma_2 p_2^\star - v_2^\star)\partial_x N^\beta(x,\xi) + v_1^\star \partial_\xi N^\beta(x,\xi) = c_2(x)N^\alpha(x,\xi), \tag{A5}$$

with the boundary conditions

$$N_1^{\alpha\alpha}(0,\xi) = N^\alpha(0,\xi), \qquad N_1^{\beta\alpha}(x,x) = -\frac{c_1(x)}{\gamma_1 p_1^\star}, \tag{A6}$$

$$N_2^{\beta\alpha}(x,x) = -\frac{c_2(x)}{\gamma_2 p_2^\star}, \qquad N_2^{\alpha\alpha}(L,\xi) = \exp\left(\frac{-L}{\tau_2 v_2^\star}\right)\frac{1}{r_2}N_2^{\beta\alpha}(L,\xi), \tag{A7}$$

$$N^\beta(x,0) = \frac{v_2^\star}{v_1^\star}N_2^{\beta\alpha}(x,0), \qquad N^\beta(0,\xi) = \delta\frac{r_2}{r_1}N_1^{\beta\alpha}(0,\xi) + (1-\delta)r_2 N^\alpha(0,\xi), \tag{A8}$$

$$N^\alpha(x,0) = \frac{v_2^\star}{v_1^\star}N_2^{\alpha\alpha}(x,0), \qquad N^\alpha(L,\xi) = \exp\left(\frac{-L}{\tau_2 v_2^\star}\right)\frac{1}{r_2}N^\beta(L,\xi). \tag{A9}$$

Equations (A1)–(A9) admit a unique solution, as proved in Reference 20. We have $N_1^{\alpha\alpha} \in \mathcal{B}(\mathcal{T}_1), N_1^{\alpha\beta} \in \mathcal{B}(\mathcal{T}_1), N_2^{\alpha\alpha} \in \mathcal{B}(\mathcal{T}_2),$ $N_2^{\alpha\beta} \in \mathcal{B}(\mathcal{T}_2),$ and $N^\alpha \in \mathcal{B}(\mathcal{T}_3), N^\beta \in \mathcal{B}(\mathcal{T}_3).$

A.2 Kernels of backstepping transformation (57)

The kernels $R_1^{\cdot\cdot}$ are defined on $\mathcal{T}_1$, the kernels $R_2^{\cdot\cdot}$ are defined on $\mathcal{T}_2$ and the kernels $R^{\cdot}$ are defined on $\mathcal{T}_3$. The transformation (57) is the inverse transformation of (51). The corresponding kernel equations are obtained differentiating equation (51) with respect to time and space, integrating by parts and injecting into (46)–(50). We obtain

$$\partial_x R_i^{ww}(x,\xi) + \partial_\xi R_i^{ww}(x,\xi) = 0, \tag{A10}$$

$$(\gamma_i p_i^\star - v_i^\star)\partial_x R_i^{vw}(x,\xi) - v_i^\star \partial_\xi R_i^{vw}(x,\xi) = 0, \tag{A11}$$

$$v_2^\star \partial_x R^w(x,\xi) - v_1^\star \partial_\xi R^w(x,\xi) = 0, \tag{A12}$$

$$(\gamma_2 p_2^\star - v_2^\star)\partial_x R^v(x,\xi) + v_2^\star \partial_\xi R^v(x,\xi) = 0, \tag{A13}$$

with the boundary conditions

$$R_1^{ww}(0,\xi) = R^w(0,\xi), \quad R_1^{vw}(x,x) = \frac{c_1(x)}{\gamma_1 p_1^\star}, \tag{A14}$$

$$R_2^{vw}(x,x) = \frac{c_2(x)}{\gamma_2 p_2^\star}, \qquad R_2^{ww}(L,\xi) = \exp\left(\frac{-L}{\tau_2 v_2^\star}\right)\frac{1}{r_2}R_2^{vw}(L,\xi), \tag{A15}$$

$$R^v(x,0) = \frac{v_2^\star}{v_1^\star}R_2^{vw}(x,0), \qquad R^v(0,\xi) = \delta\frac{r_2}{r_1}R_1^{vw}(0,\xi) + (1-\delta)r_2 R^w(0,\xi), \tag{A16}$$

$$R^w(x,0) = \frac{v_2^\star}{v_1^\star}R_2^{ww}(x,0), \qquad R^w(L,\xi) = \exp\left(\frac{-L}{\tau_2 v_2^\star}\right)\frac{1}{r_2}R^v(L,\xi). \tag{A17}$$

The well-posedness of equations (A10)–(A17) can be shown adjusting the proof of Reference 20. We have $R_1^{ww} \in \mathcal{B}(\mathcal{T}_1),$ $R_1^{vw} \in \mathcal{B}(\mathcal{T}_1), R_2^{ww} \in \mathcal{B}(\mathcal{T}_2), R_2^{vw} \in \mathcal{B}(\mathcal{T}_2),$ and $R^w \in \mathcal{B}(\mathcal{T}_3), R^v \in \mathcal{B}(\mathcal{T}_3).$

A.3 Kernels of backstepping transformation (58)

The kernels K_1^{vw} and K_1^{vv} are defined on $\mathcal{T}_2$, the kernels K_2^{vw} and K_2^{vv} are defined on $\mathcal{T}_1$, and the kernels K^w and K^v are defined on $\mathcal{T}_3$ (see notation section). The objective is to map the observer system (37)–(41) to the target system (59)–(63). Differentiating equation (58) with respect to time and space, and integrating by parts, we obtain the following set of kernel equations

$$(\gamma_1 p_1^\star - v_1^\star)\partial_x K_1^{vw}(x,\xi) - v_1^\star \partial_\xi K_1^{vw}(x,\xi) = c_1(\xi)K_1^{vv}(x,\xi), \tag{A18}$$

$$(\gamma_2 p_2^\star - v_2^\star)\partial_x K_2^{vw}(x,\xi) - v_2^\star \partial_\xi K_2^{vw}(x,\xi) = -c_2(\xi)K_2^{vv}(x,\xi), \tag{A19}$$

$$\partial_x K_i^{vv}(x,\xi) + \partial_\xi K_i^{vv}(x,\xi) = 0, \tag{A20}$$

$$\left(\gamma_1 p_1^\star - v_1^\star\right)\partial_x K^v(x,\xi) - \left(\gamma_2 p_2^\star - v_2^\star\right)\partial_\xi K^v(x,\xi) = 0, \tag{A21}$$

$$\left(\gamma_1 p_1^\star - v_1^\star\right)\partial_x K^w(x,\xi) + v_2^\star \partial_\xi K^w(x,\xi) = c_2(\xi)K^v(x,\xi), \tag{A22}$$

with the boundary conditions

$$K_1^{vv}(x,0) = \frac{v_2^\star}{v_1^\star}\delta K^v(x,0), \quad K_1^{vw}(x,x) = -\frac{c_1(x)}{\gamma_1 p_1^\star}, \tag{A23}$$

$$K_2^{vw}(x,x) = -\frac{c_2(x)}{\gamma_2 p_2^\star}, \quad K_2^{vv}(x,L) = -\exp\left(\frac{-L}{\tau_2 v_2^\star}\right)K_2^{vw}(x,L), \tag{A24}$$

$$K^w(0,\xi) = \frac{r_1}{\delta r_2}K_2^{vw}(0,\xi), \quad K^w(x,0) = -(1-\delta)K^v(x,0) + \frac{v_1^\star}{v_2^\star}K_1^{vw}(x,0), \tag{A25}$$

$$K^v(0,\xi) = \frac{r_1}{\delta r_2}K_2^{vv}(0,\xi), \quad K^v(x,L) = -\exp\left(\frac{-L}{\tau_2 v_2^\star}\right)K^w(x,L). \tag{A26}$$

It has been shown in Reference 20 that the kernels equations (A18)–(A26) admit a unique solution. We have $K_1^{vw} \in \mathcal{B}(\mathcal{T}_2)$, $K_1^{vw} \in \mathcal{B}(\mathcal{T}_2)$, $K_2^{vw} \in \mathcal{B}(\mathcal{T}_1)$, $K_2^{vv} \in \mathcal{B}(\mathcal{T}_1)$, and $K^w \in \mathcal{B}(\mathcal{T}_3)$, $K^v \in \mathcal{B}(\mathcal{T}_3)$.

A.4 Kernels of backstepping transformation (68)

The kernels $L_2^{..}$ are defined on $\mathcal{T}_1$, the kernels $L_1^{..}$ are defined on $\mathcal{T}_2$ and the kernels $L^{.}$ are defined on $\mathcal{T}_3$. The transformation (68) is the inverse transformation of (58). The corresponding kernel equations are obtained differentiating equation (68) with respect to time and space, integrating by parts and injecting into (37)–(41). We obtain

$$(\gamma_i p_i^\star - v_i^\star)\partial_x L_i^{\beta\alpha}(x,\xi) - v_i^\star \partial_\xi L_i^{\beta\alpha}(x,\xi) = 0, \tag{A27}$$

$$\partial_x L_i^{\beta\beta}(x,\xi) + \partial_\xi L_i^{\beta\beta}(x,\xi) = 0, \tag{A28}$$

$$\left(\gamma_1 p_1^\star - v_1^\star\right)\partial_x L^\beta(x,\xi) - \left(\gamma_2 p_2^\star - v_2^\star\right)\partial_\xi L^\beta(x,\xi) = 0, \tag{A29}$$

$$\left(\gamma_1 p_1^\star - v_1^\star\right)\partial_x L^\alpha(x,\xi) + v_2^\star \partial_\xi L^\alpha(x,\xi) = 0, \tag{A30}$$

with the boundary conditions

$$L_1^{\beta\beta}(x,0) = \frac{v_2^\star}{v_1^\star}\delta L^\beta(x,0), \quad L_1^{\beta\alpha}(x,x) = -\frac{c_1(x)}{\gamma_1 p_1^\star}, \tag{A31}$$

$$L_2^{\beta\alpha}(x,x) = -\frac{c_2(x)}{\gamma_2 p_2^\star}, \quad L_2^{\beta\beta}(x,L) = -\exp\left(\frac{-L}{\tau_2 v_2^\star}\right)L_2^{\beta\alpha}(x,L), \tag{A32}$$

$$L^\alpha(0,\xi) = \frac{r_1}{\delta r_2}L_2^{\beta\alpha}(0,\xi), \quad L^\alpha(x,0) = -(1-\delta)L^\beta(x,0) + \frac{v_1^\star}{v_2^\star}L_1^{\beta\alpha}(x,0), \tag{A33}$$

$$L^\beta(0,\xi) = \frac{r_1}{\delta r_2}L_2^{\beta\beta}(0,\xi), \quad L^\beta(x,L) = -\exp\left(\frac{-L}{\tau_2 v_2^\star}\right)L^\alpha(x,L). \tag{A34}$$

The well-posedness of Equations (A33) and (A34) can be shown adjusting the proof of Reference 20. We have $L_1^{\beta\beta} \in \mathcal{B}(\mathcal{T}_2)$, $L_1^{\beta\alpha} \in \mathcal{B}(\mathcal{T}_2)$, $L_2^{\beta\alpha} \in \mathcal{B}(\mathcal{T}_1)$, $L_2^{\beta\beta} \in \mathcal{B}(\mathcal{T}_1)$, and $L^\alpha \in \mathcal{B}(\mathcal{T}_3)$, $L^\beta \in \mathcal{B}(\mathcal{T}_3)$.